AD-A164 127 TWO-DIMENSIONAL HEAT CONDUCTION IN METAL FLUID COMPOSITES(U) NAVAL POSTGRADUATE SCHOOL MONTEREY CA M A GOMORI DEC 85 1/1

UNCLASSIFIED F/G 13/1 NL

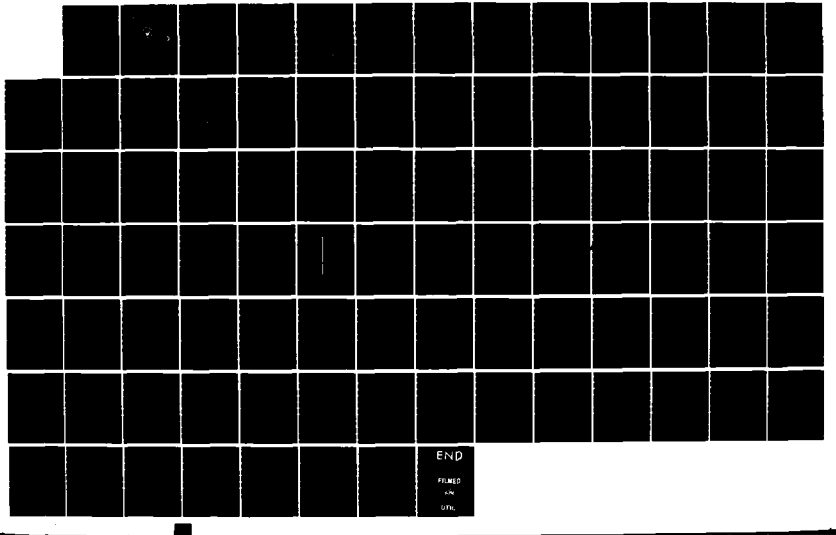

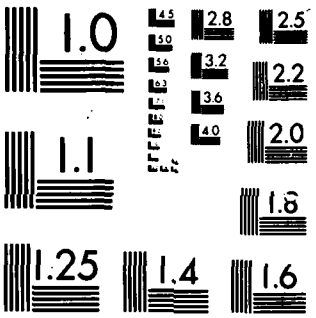

MICROCOPY RESOLUTION TEST CHART
NATIONAL BUREAU OF STANDARDS-1963-A

(2)

NAVAL POSTGRADUATE SCHOOL
Monterey, California

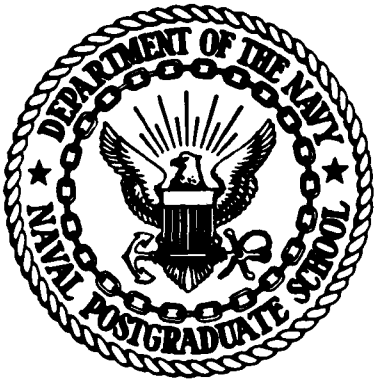

THESIS

TWO-DIMENSIONAL HEAT CONDUCTION
IN METAL, FLUID COMPOSITES

by

Michael Andrew Gomori

December 1985

Thesis Advisors: A.D. Kraus
A.S. Wanniarachchi

Approved for public release; distribution is unlimited

UNCLASSIFIED
SECURITY CLASSIFICATION OF THIS PAGE

ADA 164127

REPORT DOCUMENTATION PAGE

1a REPORT SECURITY CLASSIFICATION	1b. RESTRICTIVE MARKINGS
2a SECURITY CLASSIFICATION AUTHORITY	3 DISTRIBUTION / AVAILABILITY OF REPORT Approved for Public Release;
2b DECLASSIFICATION / DOWNGRADING SCHEDULE	Distribution is unlimited
4 PERFORMING ORGANIZATION REPORT NUMBER(S)	5. MONITORING ORGANIZATION REPORT NUMBER(S)
6a. NAME OF PERFORMING ORGANIZATION: Naval Postgraduate School; 6b OFFICE SYMBOL (If applicable): 69	7a. NAME OF MONITORING ORGANIZATION: Naval Postgraduate School
6c ADDRESS (City, State, and ZIP Code): Monterey, California 93943-5100	7b. ADDRESS (City, State, and ZIP Code): Monterey, California 93943-1500
8a NAME OF FUNDING / SPONSORING ORGANIZATION; 8b OFFICE SYMBOL (If applicable)	9. PROCUREMENT INSTRUMENT IDENTIFICATION NUMBER
8c ADDRESS (City, State, and ZIP Code)	10. SOURCE OF FUNDING NUMBERS: PROGRAM ELEMENT NO. / PROJECT NO. / TASK NO / WORK UNIT ACCESSION NO.

11 TITLE (Include Security Classification)
TWO-DIMENSIONAL HEAT CONDUCTION IN METAL, FLUID COMPOSITES

12 PERSONAL AUTHOR(S)
Gomori, Michael Andrew

13a TYPE OF REPORT	13b TIME COVERED	14 DATE OF REPORT (Year, Month, Day)	15 PAGE COUNT
Master's Thesis	FROM _____ TO _____	1985 December	89

16 SUPPLEMENTARY NOTATION

17 COSATI CODES			18 SUBJECT TERMS (Continue on reverse if necessary and identify by block number)
FIELD	GROUP	SUB-GROUP	Steam; Condensation; Filmwise; Tube; External Film; Heat-Transfer Coefficient; Enhancement; Two Dimensional; Numerical

19 ABSTRACT (Continue on reverse if necessary and identify by block number)

Filmwise condensation of steam on externally-finned tubes is a very complex process. Recent experiments have shown that enhancement ratios (ratio of steam-side heat-transfer coefficient to that of a smooth tube having the same diameter) exceeded the area enhancement produced by the fins. Moreover, the enhancement ratios for fully flooded tubes exceeded the values predicted by a simple, one-dimensional conduction model by a factor of 2 to 4. A new two-dimensional conduction model was developed, which showed that the one-dimensional model overpredicted the two-dimensional results for high conductivity tube-metals such as copper by as much as 13%. The two-dimensional model also showed that variations in fin thickness or spacing can result in an overprediction by the

20 DISTRIBUTION AVAILABILITY OF ABSTRACT	21. ABSTRACT SECURITY CLASSIFICATION
☒ UNCLASSIFIED/UNLIMITED ☐ SAME AS RPT ☐ DTIC USERS	Unclassified
22a NAME OF RESPONSIBLE INDIVIDUAL: Prof. Allan D. Kraus	22b TELEPHONE (Include Area Code): (408) 646-3381 / 22c. OFFICE SYMBOL: Code 69Ks

DD FORM 1473, 84 MAR — 83 APR edition may be used until exhausted. All other editions are obsolete.

SECURITY CLASSIFICATION OF THIS PAGE

#19 - ABSTRACT - (CONTINUED)

one-dimensional model of the two-dimensional results by as much as twenty-two percent.

Approved for public release; distribution is unlimited.

Two-Dimensional Heat Conduction
In Metal, Fluid Composites

by

Michael Andrew Gomori
Lieutenant, United States Navy
B.S., Fairleigh Dickenson University, 1979

Submitted in partial fulfillment of the
requirements for the degree of

MASTER OF SCIENCE IN MECHANICAL ENGINEERING

from the

NAVAL POSTGRADUATE SCHOOL
December 1985

Author: Michael Andrew Gomori
Michael Andrew Gomori

Approved by: Allan D. Kraus
Allan D. Kraus, Thesis Advisor

A. S. Wanniarachchi, Co-Advisor

P. J. Marto
Paul J. Marto, Chairman,
Department of Mechanical Engineering

John N. Dyer
John N. Dyer,
Dean of Science and Engineering

ABSTRACT

Filmwise condensation of steam on externally-finned tubes is a very complex process. Recent experiments have shown that enhancement ratios (ratio of steam-side heat-transfer coefficient to that of a smooth tube having the same diameter) exceeded the area enhancement produced by the fins. Moreover, the enhancement ratios for fully flooded tubes exceeded the values predicted by a simple, one-dimensional conduction model by a factor of 2 to 4. A new two-dimensional conduction model was developed, which showed that the one-dimensional model overpredicted the two-dimensional results for high conductivity tube-metals such as copper by as much as 13%. The two-dimensional model also showed that variations in fin thickness or spacing can result in an overprediction by the one-dimensional model of the two-dimensional results by as much as twenty-two percent.

TABLE OF CONTENTS

LIST OF TABLES

LIST OF FIGURES

NOMENCLATURE

A	- Area
A_f	- Total Surface Area of Finned Tube
A_s	- Smooth Tube Surface Area
D_i	- Inside Tube Diameter
D_o	- Outside Tube Diameter
e	- Fin Height
g	- Acceleration of Gravity
h_i	- Heat-Transfer Coefficient for Tube
h_o	- Heat-Transfer Coefficient for Vapor-Condensate Surface
K	- Internode Conductance Value
k_m	- Thermal Conductivity of Tube/Fin Metal
k_l	- Thermal Conductivity of Condensate
L	- Length
r_i	- Tube Inner Radius
r_o	- Tube Outer Radius
s	- Fin Spacing
t	- Fin Thickness
T	- Temperature
T_i	- Bulk Temperature of Fluid Inside Tube
T_o	- Saturation Temperature of Condensing Vapor
q	- Total Rate of Heat Transfer
q_c	- Convective Rate of Heat Transfer
q''	- Heat Flux

Q21	- Ratio of Two-Dimensional Heat Flux to One-Dimensional Heat Flux
x	- Length Coordinate
y	- Height Coordinate
z	- Height of Condensate Above Fin Tip
δ	- Depth of Node Subvolume
ρ	- Density
σ	- Surface Tension of Condensate
ϕ_1	- Ratio of the Tube Side Heat Flux with Fins Using One-Dimensional Model to Tube Side Heat Flux with Fins of Zero Thickness
ϕ_2	- Ratio of the Tube Side Heat Flux with Fins Using Two-Dimensional Model to Tube Side Heat Flux with Fins at Zero Thickness
ψ	- Condensate Retention Angle

ACKNOWLEDGEMENT

I wish to thank my wife Diane for her support during this endeavor and to my parents Andrew and Bertha whose assistance and encouragement provided the foundation for a productive and rewarding career.

I. INTRODUCTION

A. BACKGROUND

Because the size and weight of main propulsion and auxiliary systems are inversely proportional to the ease in which heat or energy is exchanged, a major thrust of the research and development program of the U.S. Navy is toward the design and development of equipment that perform at higher efficiency with a reduction in size and weight. In particular, one area of great interest is the reduction in size and weight of steam condensers.

Current equipment is of the bare or smooth tube type of heat exchanger in which the steam is condensed on the outside of the tubes (the shell side). The heat-transfer effectiveness is governed by the amount of surface and the overall resistance to the flow of heat. This overall resistance, in turn, is the sum of the vapor-side, tube wall, and water-side thermal resistances. Reduction of any or all of these resistances results in an increase in heat-transfer performance with an associated reduction in condenser surface area which translates into decreased size.

Both the vapor-side and tube-side thermal resistances can be considered as the reciprocal of the so-called hS product where h is the coefficient of heat transfer and S is the surface area through which the heat flows. Because of the curved surface of the exchanger tubing, the vapor-"space"

and tube-side surfaces are not equal and an adjustment must be made to the tube-side heat-transfer coefficient to allow for a design on the basis of the vapor or shell-side surface.

It is a fact that the vapor-side hS product (reciprocal of resistance) can be as high as two or three times the tube-side hS product. Thus, it would appear reasonable, in an attempt to decrease the overall resistance, to attack and try to increase the hS product on the tube side. Unfortunately, little can be done in the arena of increasing h significantly on either side although the vapor side has greater possibilities in this regard and, by its very location, not much can be done with regard to the increase of the tube-side surface.

It is for the foregoing reasons that recent efforts have focused on the use of externally-finned tubes in steam condensers to increase the flow of heat by increasing the vapor-side hS product [Refs. 1,2,3].

For the past few decades, it has been accepted that the use of externally-finned tubes would be inappropriate mainly because of the liquid retention (flooding) that occurs between fins (Figure 1.1). This flooding is a result of the relatively high surface tension of water (at 50°C water has a surface tension of 0.068 N/m, while refrigerants possess values about 0.015 N/m). One of the unavoidable results of flooding is the considerably lower heat transfer through the flooded portion than that through the unflooded portion. For the case of an externally finned copper tube with steam as the condensate,

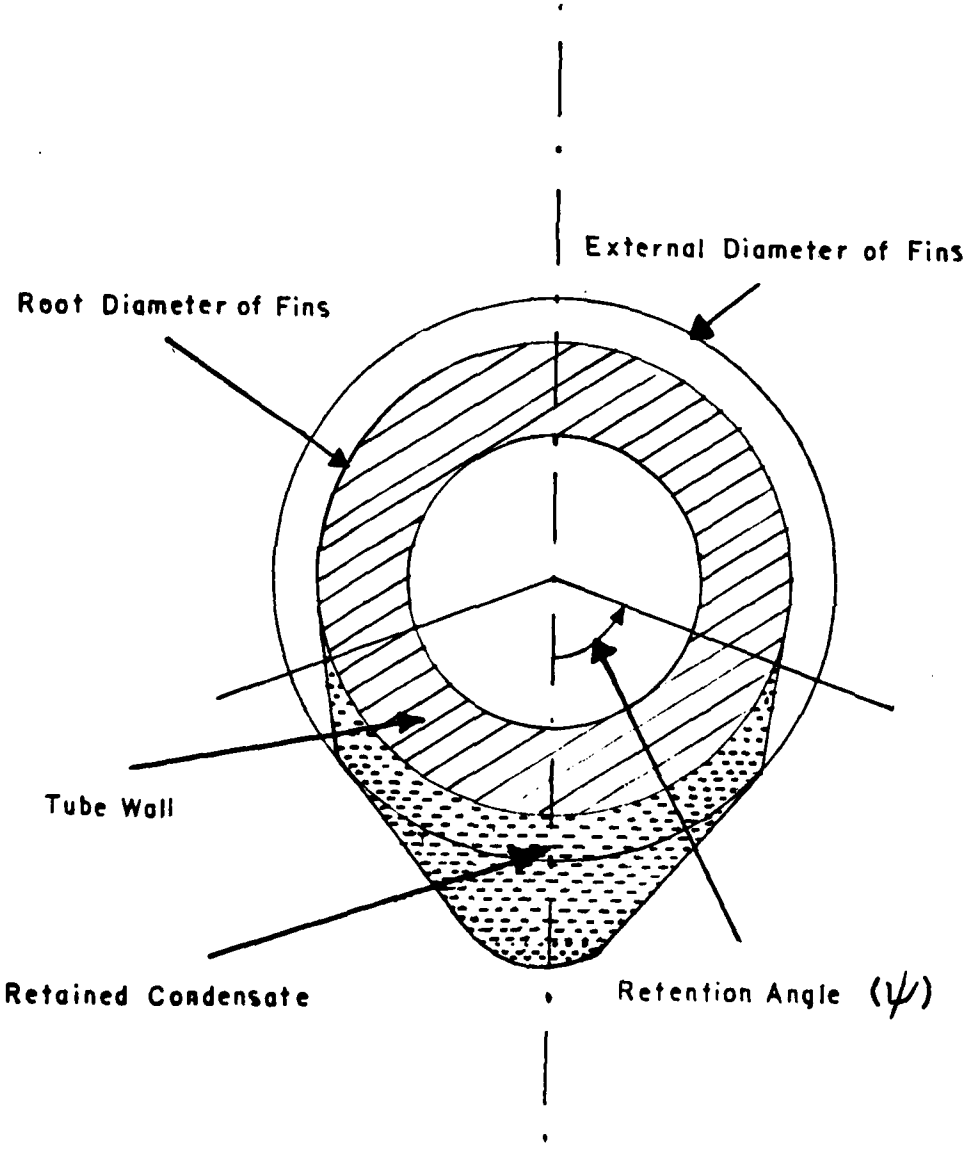

Figure 1.1. Schematic of Condensate Retention on Finned Tubes

the copper has a thermal conductivity 600 times greater than that of water (385 W/m·K for copper compared with 0.6 W/m·K for water). Due to its overall importance in the heat-transfer scheme, the flooding of the lower portion of the tube by condensate has been studied theoretically and experimentally by several investigators [Refs. 4,5,6,7,8]. These studies have shown that the flooding angle depends mainly on the fin spacing and the ratio of surface tension to density of condensate as given by the following equation for the case of rectangular-section fins [Ref. 5]:

$$\psi = \cos^{-1} \left[1 - \frac{4\sigma}{\rho g D s}\right] \qquad (1.1)$$

Recent work by Yau et al. [Ref. 9] and Wanniarachchi et al. [Ref. 1] has shown that even in the cases with considerable flooding, the heat-transfer performance exceeds that expected on the basis of area increase due to the fins.

In 1948, Beatty and Katz [Ref. 10] developed the first model to predict the condensation heat-transfer coefficient for horizontal, externally-finned tubes. Their model ignores the existence of flooding. Although their model agrees to within 10 percent for condensing fluids possessing low surface tensions, it tends to be rather inaccurate for high-surface-tension fluids, such as water. Several other investigators, Rudy and Webb [Ref. 2] and Owen et al. [Ref. 8] attempted refinement of the Beatty and Katz model but still were unable to predict

the heat-transfer coefficient to a reasonable degree of accuracy.

Rudy and Webb used the Beatty and Katz model for the unflooded portion, while neglecting heat transfer through the flooded portion. With this modification, Rudy and Webb underpredicted data for low-surface-tension fluids by up to 50 percent. Owen et al. attempted to improve the Rudy and Webb model by allowing heat transfer through the flooded portion. In order to compute heat transfer through the flooded portion, they assumed parallel conduction paths through the fins and the condensate that is flooded in the interfin space as shown in Figure 1.2. With this modification, they improved the predictions slightly; underprediction for low-surface-tension fluids decreased to about 40 percent. However, as shown by Honda and Nozu [Ref. 11],both of these models overpredicted the steam data of Yau et al. by a factor of up to 3. The fact is that the use of Beatty and Katz model, which does not take surface tension forces into consideration for the unflooded portion, may be responsible for this large discrepancy.

The most recent and accurate attempt at modelling the problem was accomplished by Honda and Nozu [Ref. 11]. Their resulting solution, a fourth-order differential equation for the film thickness, was solved numerically subject to reasonable boundary conditions. An agreement to within ±20% was achieved by their model in predicting data experimentally obtained

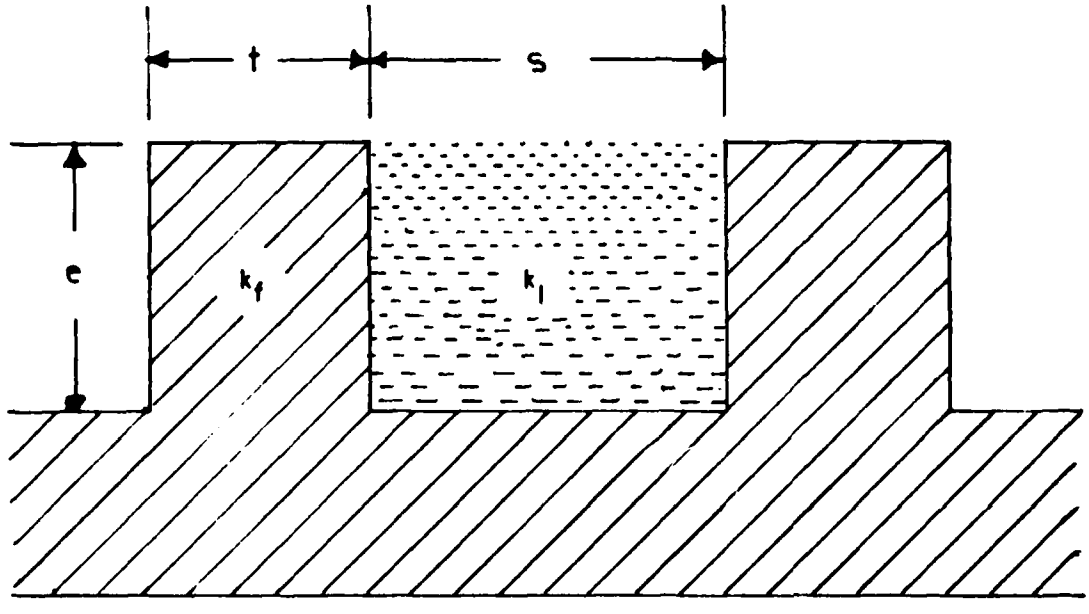

Fin Resistance $\frac{e}{k_f t}$ Liquid Resistance $\frac{e}{k_l s}$

One Dimensional Effective Resistance $\frac{e}{\frac{(k_f t + k_l s)}{t+s}}$

Figure 1.2. One-Dimensional Parallel Conduction Model

for 11 fluids and 22 tubes. However, the disagreement with steam condensation data was as high as 40%.

To understand the condensing heat transfer performance more clearly, it is convenient to define the enhancement ratio as proposed by Wanniarachchi et al. [Refs. 1,2]. The enhancement ratio is defined as the ratio of the steam-side heat-transfer coefficient of a finned tube to that of a smooth tube with the same diameter as the finned tube root diameter at the same heat flux.

The present investigator has been mainly motivated by the heat transfer through a finned tube that is completely flooded by condensate. As shown by Winniarachchi et al. [Ref. 2], a finned tube with a fin spacing of 0.5 mm, and a height and thickness of 1.0 mm and 1.0 mm respectively showed a considerable improvement in heat-transfer performance even though this tube was completely flooded by condensate. In fact, this tube showed an enhancement ratio of about 2.5 under vacuum (85 mmHg) and 4.5 at atmospheric pressure. These ratios even exceeded the area enhancement (A_f/A_s), which was 2.11. If one-dimensional conduction is assumed (see Owen [Ref. 8]), the expected enhancement ratio was computed to be about 0.8. This unexpectedly high enhancement ratio may be, at least in part, explained by two-dimensional conduction and convection in the interfin space.

B. OBJECTIVES

The main objectives of this thesis are:

1. Develop a two-dimensional numerical model of a horizontal-finned tube fully flooded with steam condensate. The program using the model shall be interactive to allow different cases of fin thickness, fin spacing, and tube-metal thermal conductivity to be studied,

2. Using a thermal analyzer computer program, determine the temperature distribution plots and heat flux for each case,

3. Compute enhancement ratios for each one of the cases studied and compare these ratios with those computed by using a one-dimensional model,

4. Compare the one and two-dimensional enhancement ratios and comment on the importance of the role of two-dimensional heat transfer in the overall heat-transfer performance,

5. Determine the value and usefulness of the two-dimensional model as an aid in the prediction of enhancement ratios for various cases.

II. DEVELOPMENT OF THE TWO DIMENSIONAL MODEL

A. THE PRINCIPLE OF THE FINITE DIFFERENCE

1. Establishment of the Spatial Increment

Consider the three-dimensional Laplace steady-state equation for the spatial temperature distribution in a configuration

$$\frac{\partial^2 T}{\partial x^2} + \frac{\partial^2 T}{\partial y^2} + \frac{\partial^2 T}{\partial z^2} = 0 \qquad (2.1)$$

It may be solved analytically, subject to certain boundary conditions, and the solution is called an analytical solution. The finite-difference solution is arrived at numerically and applies to a network of points called nodes, with the temperatures at the nodes being estimated. The numerical solutions obtained by analytical and finite-difference methods can be made to agree with any desired accuracy.

Consider a grid of nodes. Applications of equation (2.1) at a particular node whose temperature is T_o allows estimation of the second derivatives in terms of the temperature T_o and the six related temperatures at the adjacent nodes of the grid. In Figure 2.1 an arbitrary function $T = f(x)$ is shown which considers only the trace of $T = f_2(x)$ even though equation (2.1) shows that there will also be a functional relationship between T and y, namely, $T = f_1(y)$ and between t and z, namely, $T = f_3(z)$.

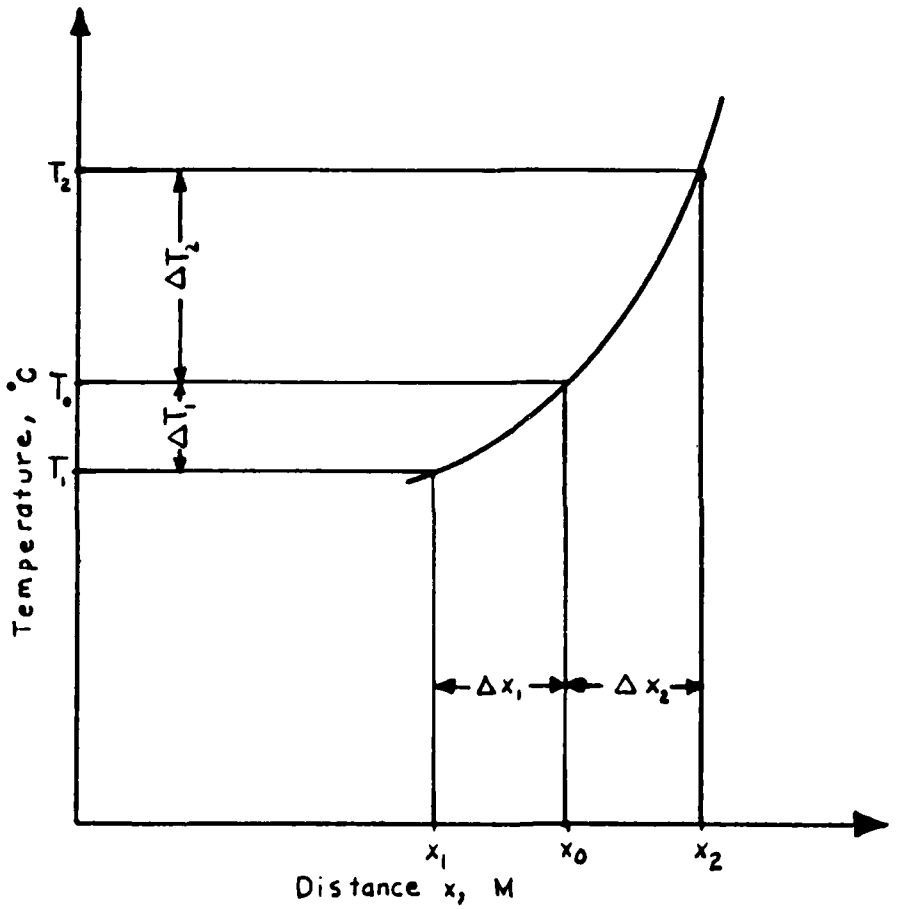

Figure 2.1. Approximation of the First Derivative

If y and z are held constant, the first derivative of equation (2.1) may be approximated by the change in T divided by the change in x:

$$\frac{\partial T}{\partial x} \approx \frac{\Delta T + \Delta T}{\Delta x_1 + \Delta x_2} = \frac{(T_2 - T_o) + (T_o - T_1)}{\Delta x_1 + \Delta x_2} = \frac{T_2 - T_1}{\Delta x_1 + \Delta x_2} \tag{2.2}$$

An estimate of the second derivative is obtained by estimating the first derivative in each of the two intervals and dividing the difference of the first derivatives by the total interval over which the first derivative estimates apply. The total interval will be the distance between the centers of the two intervals, Δx_1 and Δx_2. Hence

$$\frac{\partial^2 T}{\partial x^2} \approx \frac{\Delta T_2/\Delta x_2 - \Delta T_1/\Delta x_1}{\frac{1}{2}\Delta x_2 + \frac{1}{2}\Delta x_1}$$

If $\Delta x_1 = \Delta x_2 = \Delta x$,

$$\frac{\partial^2 T}{\partial x^2} \approx \frac{(T_2 - T_o)/\Delta x - (T_o - T_1)/\Delta x}{\Delta x} = \frac{T_1 + T_2 - 2T_o}{\Delta x} \tag{2.3}$$

A similar development using $T = f_2(y)$ with temperatures T_3 and T_4 yields

$$\frac{\partial^2 T}{\partial y^2} = \frac{T_3 + T_4 - 2T_o}{\Delta y} \tag{2.4}$$

and for $T = f_3(z)$ with temperatures T_5 and T_6

$$\frac{\partial^2 T}{\partial z^2} = \frac{T_5 + T_6 - 2T_o}{\Delta z} \qquad (2.5)$$

so that equation (2.1) may be approximated by

$$\frac{T_1 + T_2 - 2T_o}{\Delta x} + \frac{T_3 + T_4 - 2T_o}{\Delta y} + \frac{T_5 + T_6 - 2T_o}{\Delta z} = 0 \qquad (2.6)$$

and if $\Delta x = \Delta y = \Delta z$, the result is

$$T_1 + T_2 + T_3 + T_4 + T_5 + T_6 - 6T_o = 0$$

Further justification of the result indicated by equation (2.3) comes from a consideration of a Taylor Series Expansion. Recall that the Taylor Series Expansion is given by

$$f(x) = \frac{f(a)}{0!}(x-a)^0 + \frac{f'(a)}{1!}(x-a) + \frac{f''(a)}{2!}(x-a)^2 + \frac{f'''(a)}{3!}(x-a)^3 + \ldots + \frac{f^n(a)}{n!}(x-a)^n \qquad (2.7)$$

Two cases will be examined. First for $f(x) = T(x)$ at $x = x_1$, then

$$T(x=x_1) = T_1$$

$$T(x=x_o) = T_o$$

$$a = x_o$$

$$x-a = \Delta x$$

and with these in equation (2.7)

$$T_1 = T_o + \left.\frac{dT}{dx}\right|_{x_o} \Delta x + \frac{1}{2}\left.\frac{d^2T}{dx^2}\right|_{x_o} \Delta x^2 + \frac{1}{6}\left.\frac{d^3T}{dx^3}\right|_{x_o} \Delta x^3 + \frac{1}{24}\left.\frac{d^4T}{dx^4}\right|_{x_o} \Delta x^4 + \ldots \qquad (2.8)$$

Then for $f(x) = T(x)$ at $x = x_2$

$$T(x=x_2) = T_2$$

$$T(x=x_o) = T_o$$

$$a = x$$

$$x-a = -\Delta x$$

With these in equation (2.7)

$$T_2 = t_o - \left.\frac{dT}{dx}\right|_{x_o} \Delta x + \frac{1}{2}\left.\frac{d^2T}{dx^2}\right|_{x_o} \Delta x^2 - \frac{1}{6}\left.\frac{d^3T}{dx^3}\right|_{x_o} \Delta x^3 + \frac{1}{24}\left.\frac{d^4T}{dx^4}\right|_{x_o} \Delta x^4 - \ldots \qquad (2.9)$$

When equations (2.8) and (2.9) are added, one obtains

$$T_2 + T_1 = 2T_o + \frac{d^2T}{dx^2}(\Delta x)^2 + \frac{1}{12}\frac{d^4T}{dx^4}(\Delta x)^4 + \ldots \qquad (2.10)$$

If Δx is small, then all terms above the second order in Eq. (2.9) may be considered negligible. Thus upon rearrangement, it is seen that

$$\left.\frac{d^2T}{dx^2}\right|_{x_o} = \frac{T_1 + T_2 - 2T_o}{\Delta x^2} \qquad (2.11)$$

which is a result that is identical to equation (2.3). Of course a similar development will provide a substantiation of equations (2.4), (2.5) and (2.6).

2. Node to Datum Analysis

Using the approximations for the second derivative, a node analysis can be performed to predict the temperature distribution in a mathematical model of a physical configuration. With a node analysis, the configuration of interest is divided into small but finite subvolumes with each subvolume being considered as isothermal. It may be then assumed that the geometric center of each subvolume is representative of that subvolume and this geometric center is called the node-point or node.

A node analysis consists of an application of the First Law of Thermodynamics to generate energy balances for each node. This is done for each node by equating

HEAT IN + HEAT GENERATED = HEAT OUT + HEAT ACCUMULATED (2.12)

For the two dimensional case displayed in Figure 2.2, the development of the node equations for node point (j,k) is shown in Figure 2.3. Assuming heat flow by conduction and a nodal dissipation, q, a steady state or First Law energy balance requires that the sum of all heat flows (Watts or BTU/hr) leaving the node equals zero. Thus with a heat input as a negative heat flow outward,

$$q_1 + q_2 + q_3 + q_4 - q_i = 0 \qquad (2.13)$$

In terms of the temperatures in Figure 2.4 and in terms of the Fourier Law

$$q = \frac{KA(\Delta T)}{L} \qquad (2.14)$$

$$q_1 = \frac{K\Delta y}{\Delta x}\,\delta(T_o - T_1)$$

$$q_2 = \frac{K\Delta x}{\Delta y}\,\delta(T_o - T_2)$$

$$q_3 = \frac{K\Delta y}{\Delta x}\,\delta(T_o - T_3)$$

$$q_4 = \frac{K\Delta x}{\Delta y}\,\delta(T_o - T_4)$$

and when these are inserted into equation (2.13), the result is

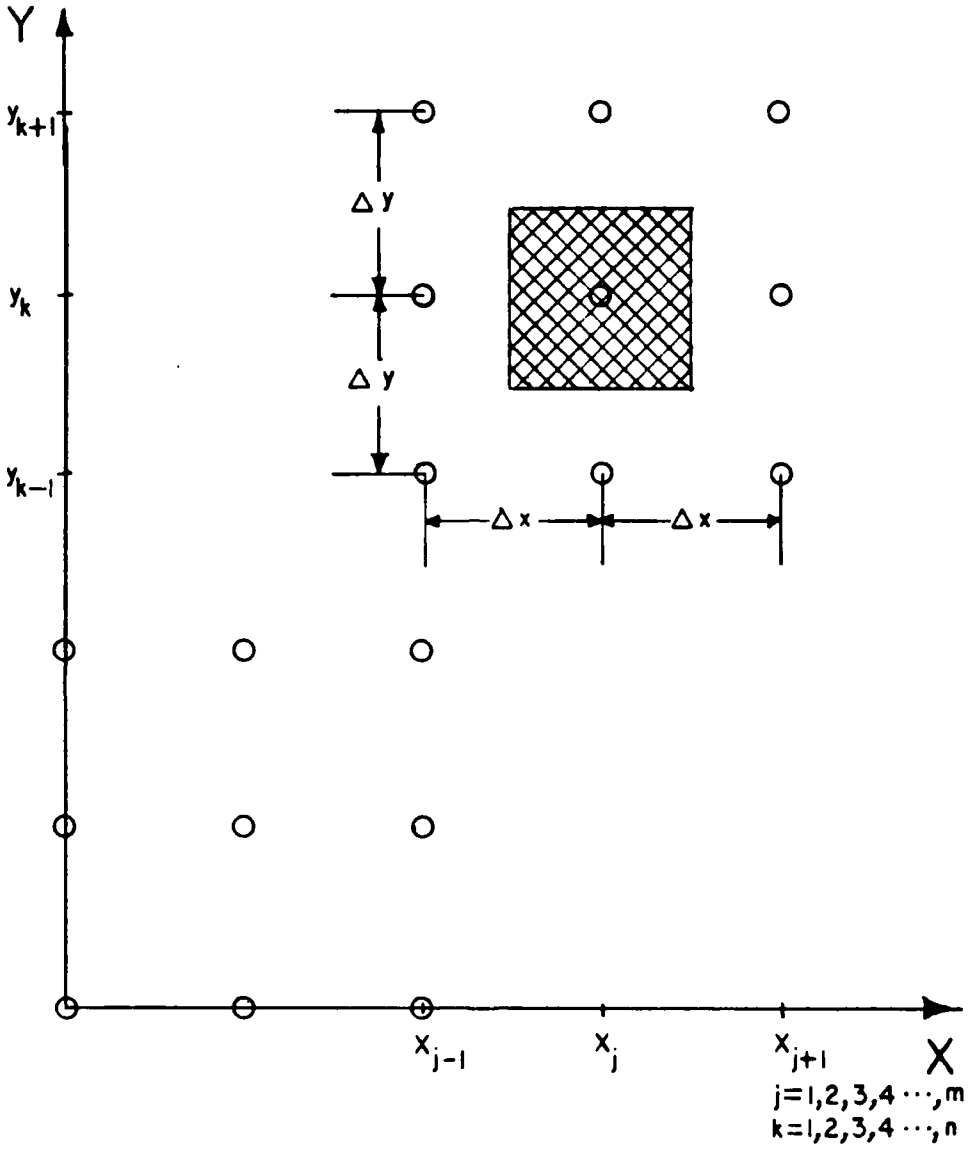

Figure 2.2. Two-Dimensional Case

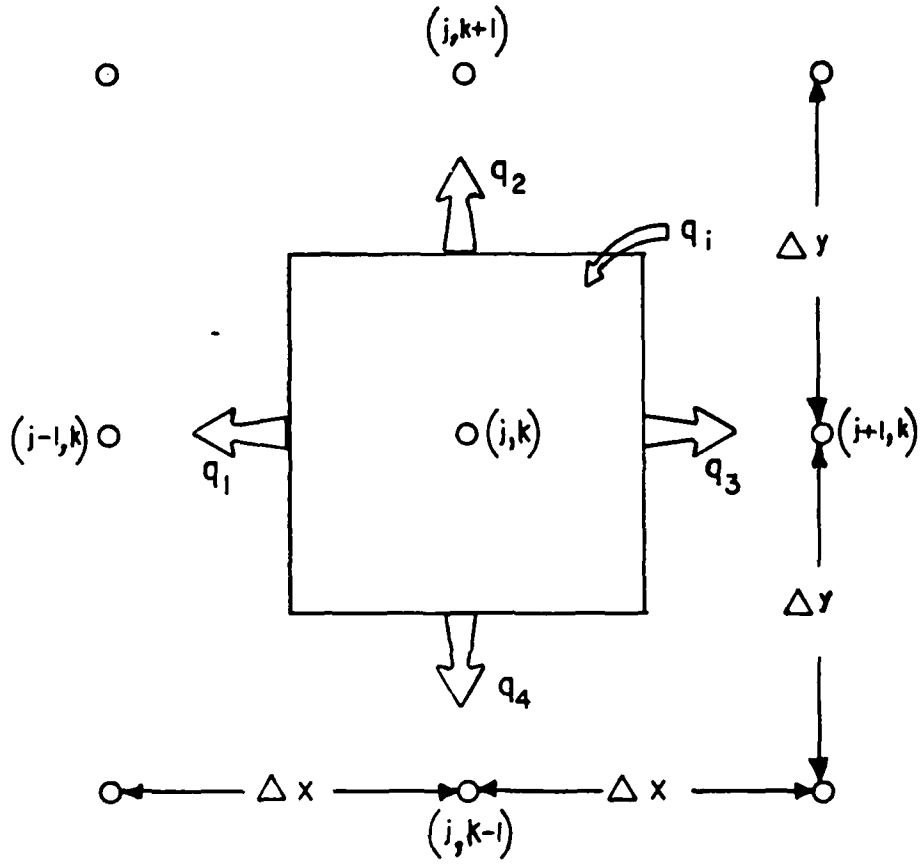

Figure 2.3. Node Equation Point (j,k)

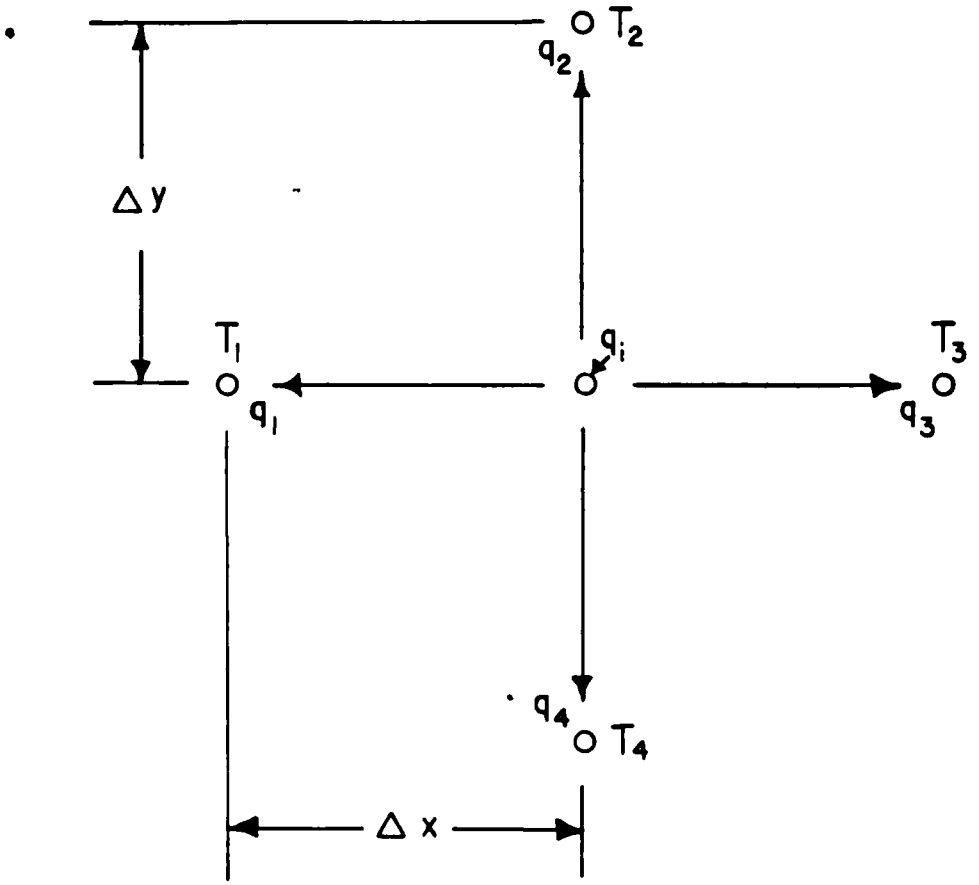

Figure 2.4. Node Equation

$$\frac{K\Delta y}{\Delta x}\,\delta(T_o-T_1) + \frac{K\Delta x}{\Delta y}\,\delta(T_o-T_2) + \frac{K\Delta y}{\Delta x}\,\delta(T_o-T_3)$$

$$+ \frac{K\Delta x}{\Delta y}\,\delta(T_o-T_4) = q_i \qquad (2.15)$$

If two conductances are defined by $K1 = K\Delta y\delta/\Delta x$ and $K2 = K\Delta x\delta/\Delta y$ then

$$K1(T_o-T_1) + K2(T_o-T_2) + K1(T_o-T_3) + K2(T_o-T_4) = q_i \qquad (2.16)$$

and if there is no heat generation ($q_i=0$), the equation becomes

$$T_o(2K1 + 2K2) - K1(T_1) - K2(T_2) - K1(T_3) - K2(T_4) = 0 \qquad (2.17)$$

For the case where there is heat flow by both conduction and convection as in Figure 2.5, with a heat input as a negative flow outward,

$$q_1 + q_2 + q_3 + q_c - q_i = 0 \qquad (2.18)$$

For the conduction terms, q_1, q_2 and q_3, equation (2.14) is still applicable. However, for the convection at the boundary as indicated by q_c (Figure 2.5)

$$q_c = h\Delta y\delta(\Delta T) \qquad (2.19)$$

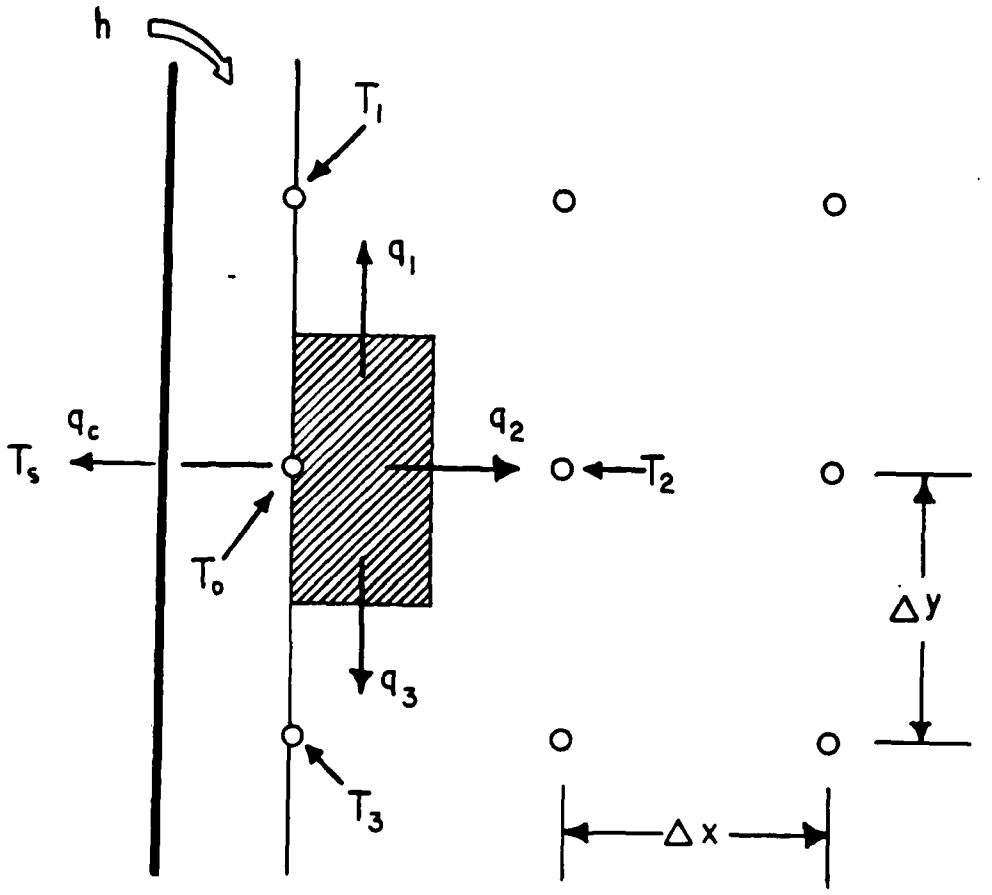

Figure 2.5. Node on Convecting Boundary

In terms of the temperatures in Figure 2.5

$$q_1 = \frac{K(\Delta x/2)}{\Delta y}\,\delta(T_o - T_1)$$

$$q_2 = \frac{K\Delta y}{\Delta x}\,\delta(T_o - T_2)$$

$$q_3 = \frac{K(\Delta x/2}{\Delta y}\,\delta(T_o - T_3)$$

$$q_c = h\Delta y\,\delta(T_o - T_s)$$

and when these are inserted into equation (2.18), the result is

$$\frac{K(\Delta x/2)}{\Delta y}\,\delta(T_o - T_1) + \frac{K\Delta y}{\Delta x}\,\delta(T_0 - T_2) + \frac{K(\Delta x/2)}{\Delta y}\,\delta(T_o - T_3) + h\Delta y\delta(T_o - T_s) = q_i \qquad (2.20)$$

Letting $K1 = \frac{K(\Delta x/2)}{\Delta y}$, $K2 = \frac{K\Delta y\delta}{\Delta x}$ and $K3 = h\Delta y\delta$, then

$$K1(T_o - T_1) + K2(T_o - T_2) + K1(T_o - T_3) + K_3(T_o - T_s) = q_i \qquad (2.21)$$

which can be simplified to

$$(2K1 + K2 + K3)T_o - K1T_1 - K2T_2 - K1T_3 = q_i \qquad (2.22)$$

and once again if there is no heat generation ($q_i = 0$), the equation becomes

$$(2K1 + K2 + K3)T_o - K1T_1 - K3T_2 - K1T_3 - K3T_s = 0 \qquad (2.23)$$

For the case of a node on an adiabatic boundary with no heat generation as in Figure 2.6

$$q_1 + q_2 + q_3 = 0 \qquad (2.24)$$

In terms of the temperature in Figure 2.6 and in terms of the Fourier Law

$$q_1 = \frac{K(\Delta x/2)}{\Delta y}\,\delta(T_o - T_1)$$

$$q_2 = \frac{K\Delta y}{\Delta x}\,\delta(T_o - T_2)$$

$$q_3 = \frac{K(\Delta x/2)}{\Delta y}\,\delta(T_o - T_3)$$

and when these are inserted into equation (2.24), the result is

$$\frac{K(\Delta x/2)}{\Delta y}\,\delta(T_o - T_1) + \frac{K\Delta y}{\Delta x}\,\delta(T_o - T_2) + \frac{K(\Delta x/2)}{\Delta y}\,\delta(T_o - T_3) = 0 \qquad (2.25)$$

Letting $K1 = \frac{K(\Delta x/2)}{\Delta y}\,\delta$ and $K2 = \frac{K\Delta y\delta}{\Delta x}$

$$(2K1 + K2)T_o - K1T_1 - K2T_2 - K1T_3 = 0 \qquad (2.26)$$

It is easy to see that when one proceeds in this manner for all nodes, an nxn set of simultaneous algebraic

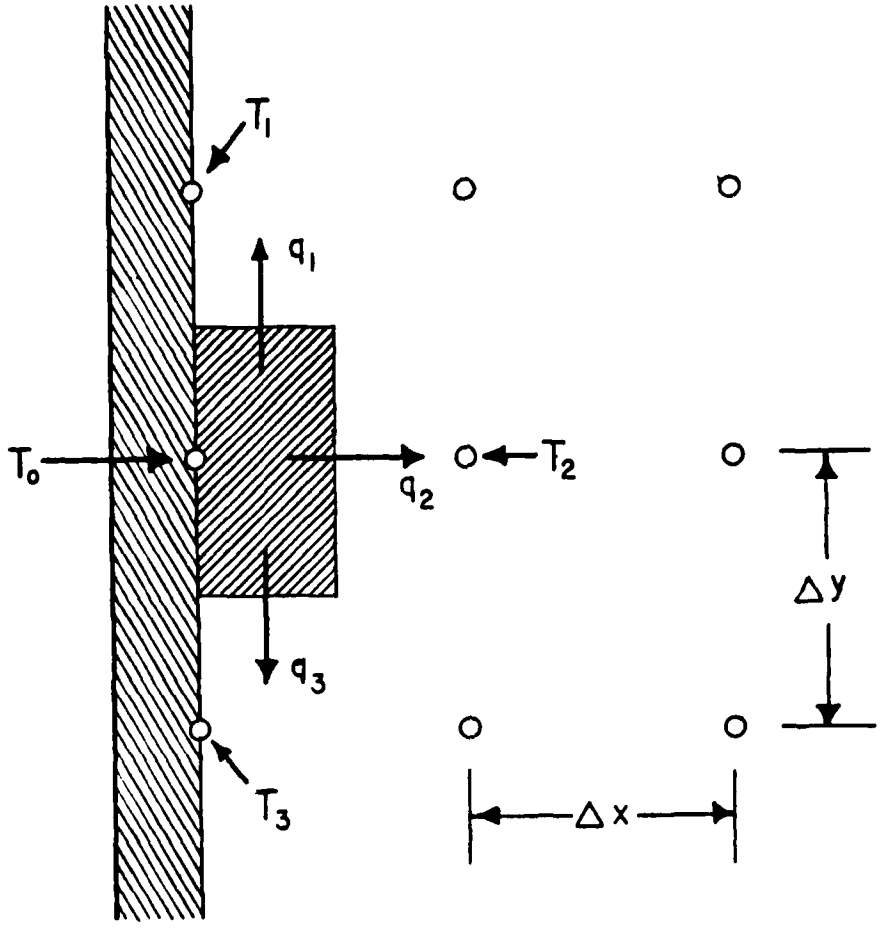

Figure 2.6. Node on Adiabatic Boundary

equations will result. These may be represented in matrix form as

$$[K][T] = [Q] \qquad (2.27)$$

where [K] is an nxn matrix of coefficients and [T] and [Q] are nxl column vectors representing the node temperatures and heat inputs respectively.

The solution of equation (2.27) is handled by the computer program TVSSI [**Ref.** 12:Appendix A].

B. MODEL BUILDER TVIN

In order to provide input to program TVSSI, it was necessary to create a model of the configuration to be analyzed. The overall model of the condensing region incorporated three major features. Because the system to be modelled was an externally finned tube with the external space flooded by condensate, the azimuthal portion of the model was chosen to be $1/2\pi$ radians. This is shown in Figure 2.7 and because the areas of each node contain a π term, the use of $1/2\pi$ simplified the construction of the node equations by permitting cancellation of the π terms. The second feature required that the maximum number of nodes to be used for the model was 300, due to input restrictions (the dimension statement) of the main thermal analyzer. The final requirement necessitated that the program be written so

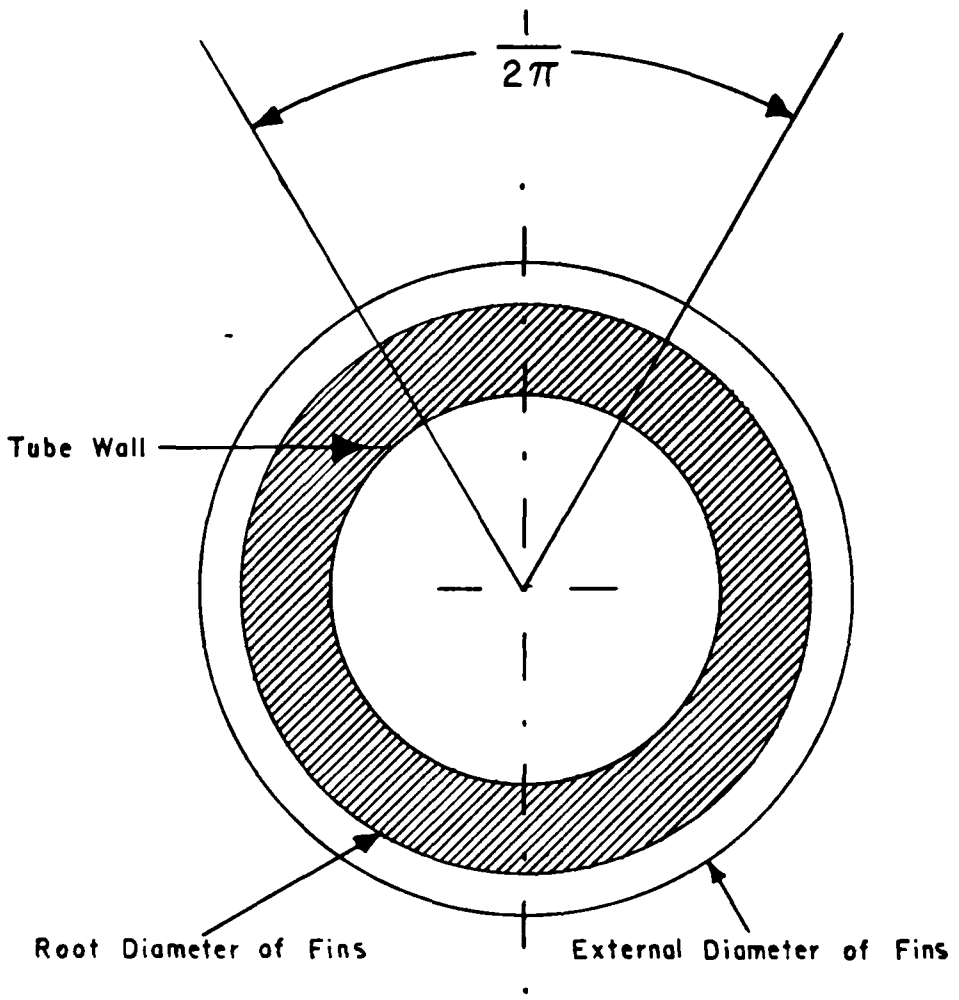

Figure 2.7. Model Azimuthal Section

as to allow the user to input the variables listed in Table I interactively.

The basic model is shown in Figure 2.8. The upper horizontal edge represents the condensate/vapor interface while the lower horizontal edge represents the inner wall of the tube. Heat-transfer coeffients were specified for the inner-tube wall and the vapor-condensate interface. The model assumes that the heat is transferred across the retained condensate by conduction only. Due to symmetry, the dotted-dashed lines at the two vertical edges of the figure represent an isolation of a fin-condensate-tube entity into a repeating section. These lines, of course, represent adiabatic boundaries. Thus, the model assumes that the only heat transferred into or out of the model occurs at either the condensate/vapor interface or the inner tube wall.

The first model constructed consisted of 299 nodes with 13 columns and 23 rows. The outermost rows and columns consisted of half node subvolumes. This facilitated the placement of the node centers at both the inner tube wall and upper condensate/vapor interface in addition to the boundary of the outer tube wall and fin perimeter. Nine rows were placed in the condensate region above the fin and in the region including the fin and adjacent condensate. The remaining four rows were placed in the tube wall region. In addition the fin region contained 4 columns of nodes while the remaining eight columns were placed in the inter-fin space.

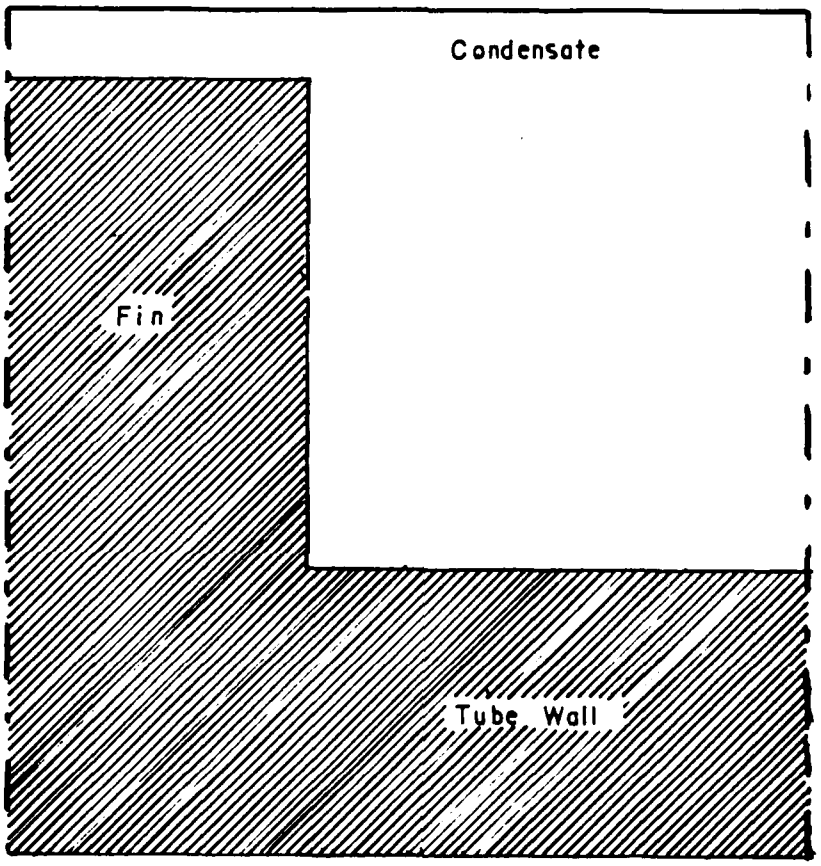

Figure 2.8. Basic Model

TABLE I

INPUT VARIABLES FOR MODEL BUILDER TVIN

T_i	- Temperature of fluid inside tube
T_o	- Temperature outside condensate layer
r_i	- Inner radius of tube
r_o	- Outer radius of tube
h_i	- Heat transfer coef. at inside tube wall
h_o	- Heat transfer coef. at condensate layer
k_m	- Thermal conductivity at tube and fin
k_l	- Thermal conductivity of condensing liquid
e	- Fin height
t	- Fin width
s	- Spacing between fins
z	- Height of condensate above tip of fin

The location of these columns and rows determined the height and width increments of the various subvolumes, depending on their location in the model. For example, if the tube wall thickness is four millimeters, and the tube wall area contains four rows, the height increment for a node in this region would be 4 mm/4 rows = 1 mm. The width increments for a node would be computed in identical fashion by dividing the size of the particular region by the number of columns occupying that region. Figure 2.9 identifies all of the different height and width increments utilized by the model.

C. EVALUATION OF RESULTS

1. Verification of Accuracy

Verification of the model consisted of using the temperatures generated by TVSSI (Using TVIN as input) and the conductance values employed in TVIN to compute the heat flow across three boundaries in the model:

(1) condensate upper surface

(2) fin perimeter and tube outer wall

(3) tube inner wall

The foregoing heat flows were computed in each case by using the node temperatures generated by TVSSI with the associated internode conductance values used in the input generated by TVIN. These heat flows, of course, must be

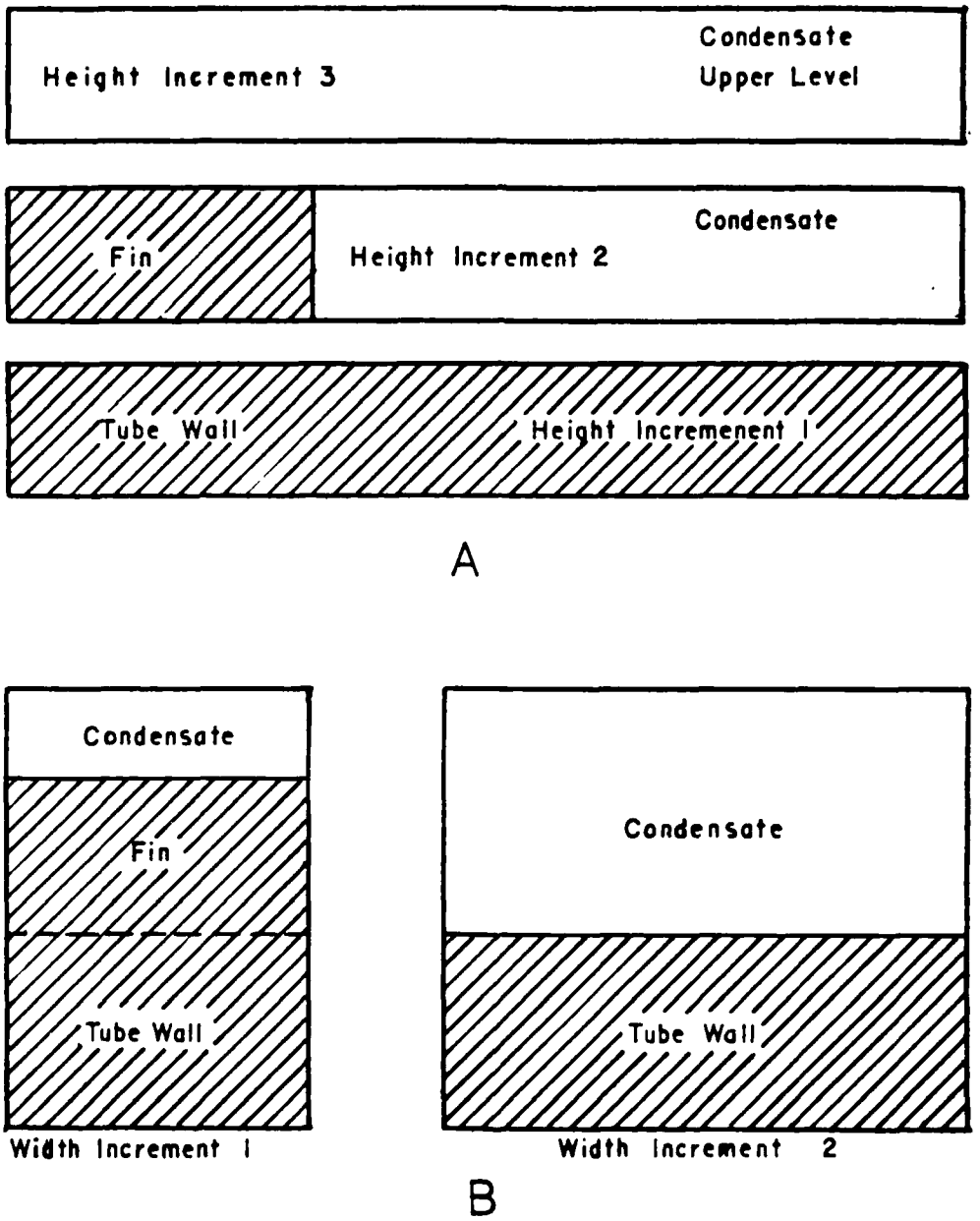

Figure 2.9. Model Increments. (A) Height and (B) Width

equal and it was observed at the outset that 13x23 model yielded certain unacceptable discrepancies in the three values.

Because the 13x23, 299 node model was found to be inaccurate, it was determined that, in order to achieve the requisite accuracy, slight adjustment of the number of rows and columns was required from run-to-run.

TVIN was reprogramed to allow flexibility in the number of rows and columns utilized in the model as well as placement of the nodes in the fin, tube or liquid regions. The first change instituted was to fix the number of rows contained in the condensate layer above the fin tip at two rows. This action was acceptable because the original height of this layer was only 0.08 mm compared with a 1.0 mm fin height and 3.175 mm tube wall thickness. Fixing the number of rows at two permitted the use of additional rows at the fin and tube levels. Program TVIN was changed to interactively accept a specified number of columns (see Appendix A). The number of rows was obtained by making the product of rows and columns as close as possible to 300.

A description of the menu-driven procedure for the selection and allocation of rows and columns for a 296-node model example now follows:

If the response to the query 'How many columns are desired?' is 8, the program will provide 300/8 = 37.5 or 37 rows. This yields an 8x37 = 296 node model.

Suppose the response to the query 'How many rows are desired for the tube wall?' is 5. Then the program will

allocate 37-5 = 32 rows for the fin and condensate layer above the fin.

However, the number of rows in the condensate layer above the fin tip is fixed at 2. Thus the number of rows in the fin becomes 32-2 = 30. The result is an 8x37, 296 node model. A display of the foregoing model set-up is shown in Figure 2.10.

2. Model Verifier Q1

As mentioned in the previous section, once an input file had been created by TVIN, and the node temperatures were calculated by the thermal analyzer, TVSSI, the solution was verified for correctness and accuracy. This check consisted merely of a comparison of the heat flow (watts) across three surfaces in the model. An error of 3.5% was established as the maximum allowable for a solution to be considered acceptable. The model verifier Program Q1 (see Appendix B), is an offshoot of the model builder TVIN as it interactively accepts the same input data required to build the model. Once all input parameters are set, the program generates and stores each inter-connecting node conductance value.

In the next step, all node temperatures computed by the thermal analyzer are read and stored, by location in the model. The node numbers of the condensate outer layer, fin perimeter and outer tube wall and the inner tube surface are determined for each model via an algorithm which requires as

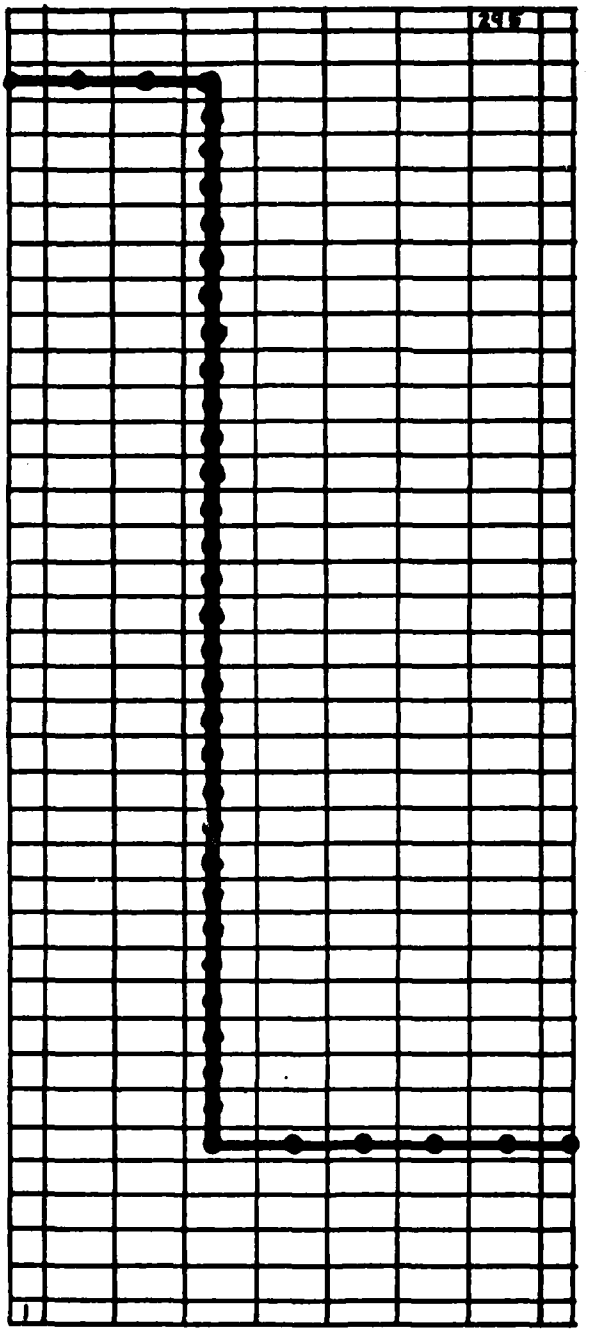

Figure 2.10. 8x37, 296 Node Model

input, the number of columns and rows being used in the model along with their placement. In addition to determining the nodes on these surfaces, the algorithm also computes the node number of each of the adjoining nodes in the direction of the heat flow. Computation of the heat flow by program Q1 is then simply a matter of taking each surface node conductance and multiplying it by the temperature difference between the surface node and its adjoining node. The summation of all the surface node values results in the total heat flow across the particular surface.

D. THERMAL ANALYZER TVSSI

The computer program TVSSI used in obtaining the temperature distributions was adapted from program TVSS2 listed by Kern and Kraus [Ref. 13:Appendix 2a]. This adaptation consisted of modifying TVSS2 to compute solutions in the SI system and accept an input file specifically designed by model builder TVIN for each externally finned tube case. This program also had to be adapted to the IBM 3033 AP system.

The program utilizes the Cholesky decomposition scheme, and because of the linearization of the radiation terms (not used in this study), the program is iterative. A more indepth description of the Cholesky Scheme pertaining to the program is discussed by O'Hare [Ref. 12:pp. 48-52].

For all the cases which were studied, the following parameters were set for the analyzer:

1. The initial temperatures at which all nodes were set and at which the computer began the iterative process was 100°C.

2. An eventual accuracy of .05 between the final and next to last iterations was used.

3. A radiation coefficient convergence factor 0f 0.66667 between iterations was used. This is required by the program even if radiation is not considered as a mode of heat transfer in the model.

4. The maximum number of iterations that the computer was allowed to perform was set at 12 to avoid excessive computer running time.

5. A damping factor of 0.8 was set as an initial damping factor based on the number of non-linear terms in all of the node equation.

The ability of TVSSI to correctly solve a numerical model was verified by providing as input a data set listed by Kern and Kraus [Ref. 13:pp. 326-336] for an extended surface problem where the solutions were derived analytically. The computer generated solution agreed completely with the analytic solution thereby assuring confidence of analyzer generated temperatures.

III. RESULTS AND DISCUSSION

A. INTRODUCTION

During this thesis effort, 15 different cases were studied using the programs TVIN and TVSSI. Table II lists the parameters that remained constant in all cases. A summary of all cases examined and their results are listed in Table III.

B. SMOOTH-TUBE EVALUATION

As a method for comparison of the variation in heat-transfer performance, the heat flux for a smooth tube with the same diameter as the finned-tube root diameter was established as a baseline value. The ratio of the one- and two-dimensional heat fluxes to the heat flux of the finned tube with fin width approaching zero were designated ϕ_1 and ϕ_2 respectively. The equation used to determine the finned-tube of zero fin width heat flow is given by:

$$Q = \frac{(T_o - T_1)}{\frac{D_o}{(h_1)(D_1)} + \frac{D_o(\ln(D_o/D_1))}{2k_m} + \frac{e}{k_1} + \frac{1}{h_o}} \qquad (3.1)$$

C. ONE DIMENSIONAL HEAT FLOW

The one-dimensional model utilized in this study assumed, as did Owen et al. [Ref. 8], parallel paths for heat flow across the tube wall, fin and retained condensate. Furthermore, a simplifying assumption was made that heat flow is purely radial and that the heat is transferred across the retained condensate

TABLE II

CONSTANT PARAMETERS FOR MODEL BUILDING PROGRAM TVIN

h_i = 30000 W/m·K

h_o = 100000 W/m·K

r_i = 6.35 mm

r_o = 9.525 mm

e = 1.0 mm

K_l = 0.6 W/m·K

T_o = 48.0 °C

T_l = 22.0 °C

TABLE III

SUMMARY OF CONFIGURATIONS EXAMINED WITH HEAT TRANSFER PERFORMANCE

CASE	K m	Fin Width t (mm)	Inter-Fin Spacing s (mm)	ϕ_1	ϕ_2	A_f / A_s	ϕ_2/ϕ_1	q'' 1D (W/m^2)	q'' 2D (W/m^2)
1	385	1.00	.5	14.74	13.02	2.46	.882	.29458	.18057
2	385	1.00	1.0	10.95	10.44	2.09	.954	.15195	.14488
3	385	1.00	1.5	9.12	9.05	1.87	.993	.12651	.12561
4	385	.50	.5	11.39	11.89	3.14	1.04	.15801	.16504
5	385	.50	.5	8.04	10.35	3.82	1.29	.11159	.14362
6	45	1.00	.5	9.14	8.98	2.46	.982	.12186	.11968
7	45	1.00	1.0	7.11	7.76	2.09	1.09	.09486	.10346
8	45	1.00	1.5	6.02	6.86	1.87	1.18	.09027	.09146
9	45	.50	.5	7.05	8.29	3.14	1.17	.09397	.11055
10	45	.25	.5	5.55	7.55	3.82	1.30	.07701	.10078
11	16	1.00	.5	5.66	5.86	2.46	1.03	.06985	.07244
12	16	1.00	1.0	4.52	5.19	2.09	1.14	.05573	.06409
13	16	1.00	1.5	3.97	4.67	1.87	1.17	.04893	.05771
14	16	.50	.5	4.54	5.48	3.14	1.20	.05609	.06772
15	16	.25	.5	3.72	5.34	3.82	1.30	.04594	.06047

by conduction only. This was accomplished by modifying program TVIN in such a way so that the data file it created contained only those internode conductance values representing heat flow in the radial direction while deleting those conductance terms pertaining to axial heat flow. Programs TVSSI and Q1 were utilized to compute the node temperatures and heat flow for each case. Once again, a maximum error of 3.5% was used when heat flows generated by program Q1 were verified.

D. TWO DIMENSIONAL HEAT FLOW

The heat flow for the two-dimensional case was evaluated by the methods discussed in Chapters I and II.

E. EFFECTS OF FIN SPACING AND FIN WIDTH ON PERFORMANCE

Heat fluxes were computed for five different cases of fin width and spacing. Three cases had a fin width of 1 mm with spacings of 0.5, 1.0 and 1.5 mm respectively. The other two cases held the spacing constant at 0.5 mm, while the fin width was adjusted to 0.5 and 0.25 mm.

1. Effects of Fin Spacing

This section presents results showing the variations of heat flux having fin spacing as a parameter. Figures 3.1, 3.2 and 3.3 present results for tubes having a fin width of 1.0 mm with fin spacings of 0.5, 1.0 and 1.5 mm. Each figure represents the same spacing variation with the tube-metal thermal conductivity being varied from 385.0 W/m.K for copper, through 45.0 W/m K for copper-nickel, down to 16.0 W/m·K for the case of

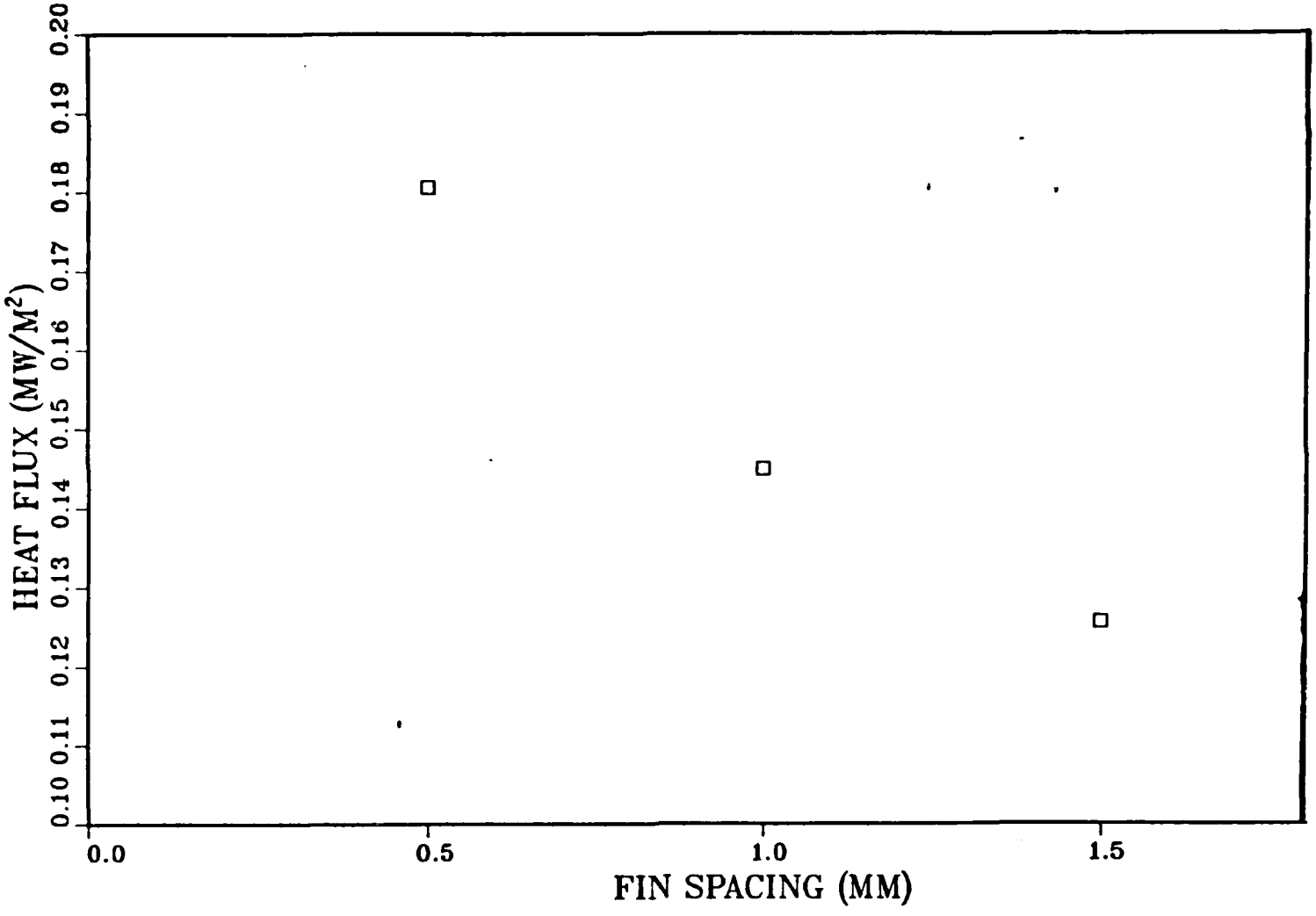

Figure 3.1. Predicted Heat-Transfer Performance of Finned Copper Tube with e = 1.0 mm and t = 1.0 mm

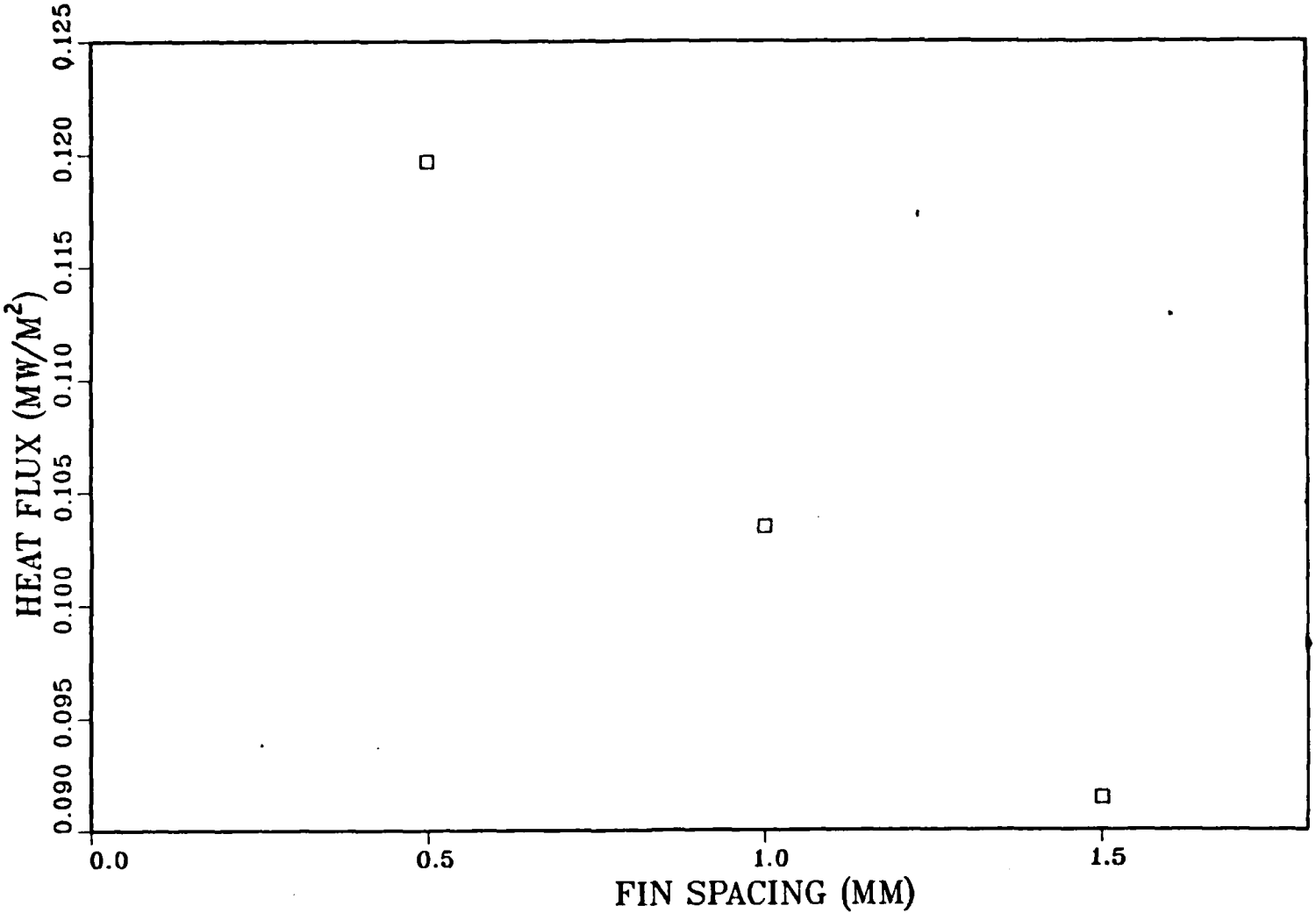

Figure 3.2. Predicted Heat-Transfer Performance of Finned Copper-Nickel Tube With e = 1.0 mm and t = 1.0 mm

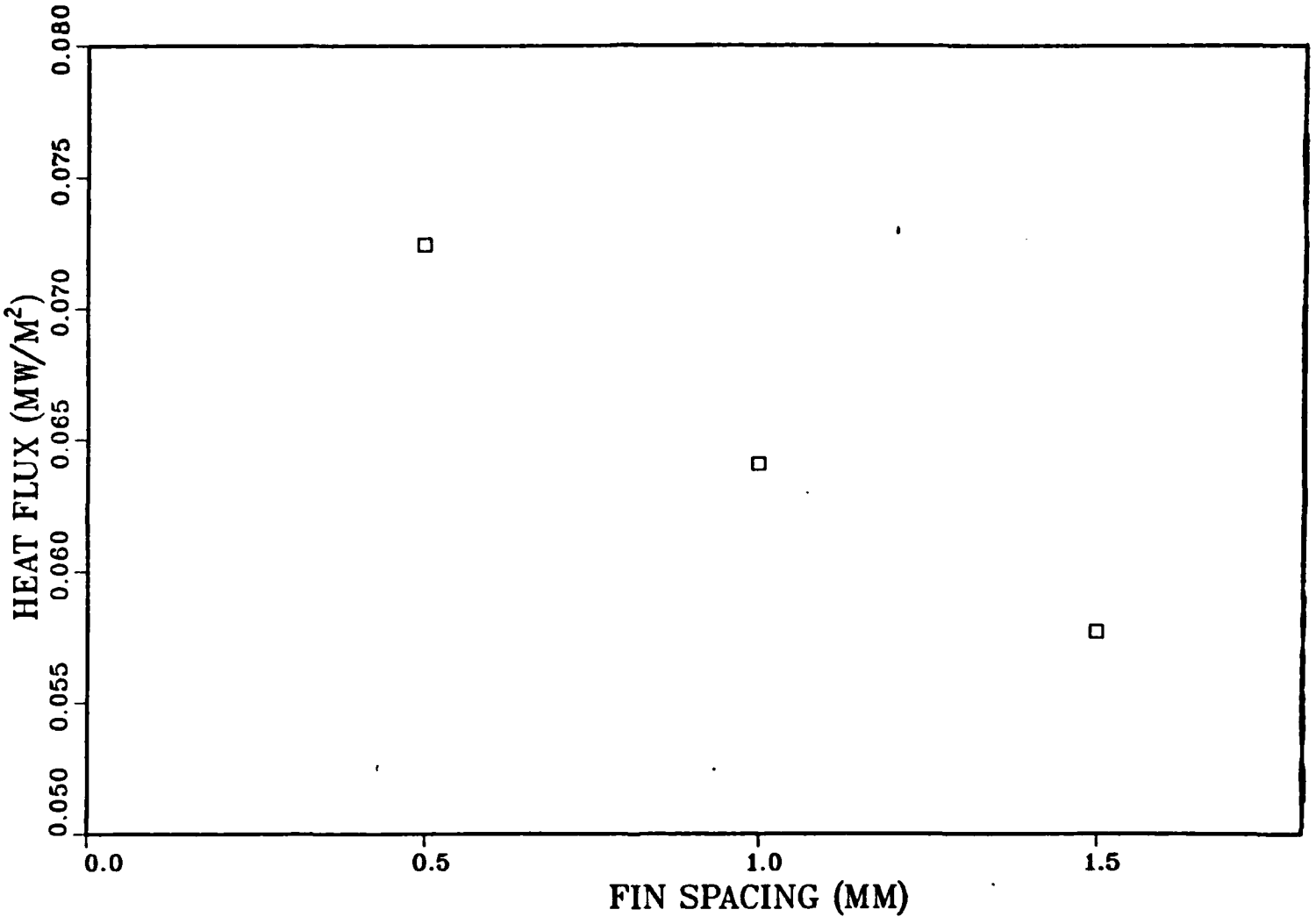

Figure 3.3. Predicted Heat-Transfer Performance of Finned Stainless Steel Tube With e = 1.0 mm and t = 1.0 mm

stainless steel. Similarly, Figures 3.4, 3.5 and 3.6 present the ratio of the two-dimensional heat flux to the one-dimensional heat flux (Q21). For each case of tube-metal thermal conductivity, the fin spacing of 0.5 mm shows the best heat-transfer performance, while the worst performance occurs at a spacing of 1.5 mm. Figures 3.7, 3.8 and 3.9 present isotherm plots for all three cases of thermal conductivity for the finned tube have a 0.5 mm fin spacing and 1.0 mm fin width. Moreover, the ratio Q21 has its smallest value at a find spacing of 0.5 mm and increases with increasing fin spacing. Enhancement ratios for the various cases had their maximum value at the 0.5 mm fin spacing and this ratio showed a marked decreaase as the fin spacing was increased.

The results indicate several important facts. The first and most important is the significant role the two-dimensional heat flow plays in this type of extended surface analysis. The increasing Q21 ratio with increasing fin spacing shows that for the cases of copper and copper-nickel tube-metal, the axial heat flow into the fin upper side surface tends to raise the temperature of the fin tip resulting in a choking effect of the heat flow into the fin tip surface. This is of enormous consequence because in each and every case, the majority of the he absorbed by the finned tube is accomplished at the fin tip. Because the one-dimensional case allows no axial heat flow into the fin side surface, a greater temperature gradient occurs at the fin tip resulting in a greater heat flow. As the

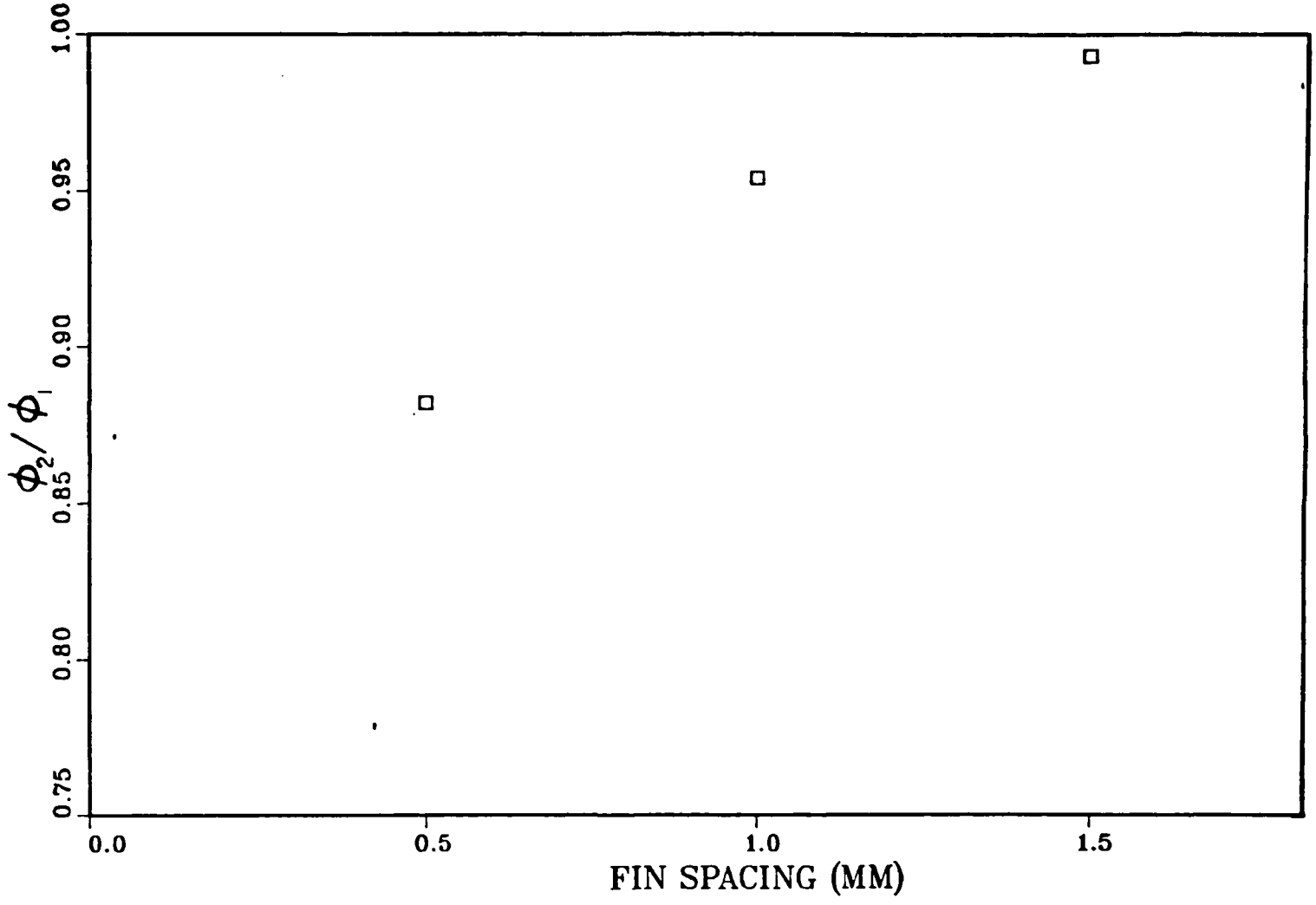

Figure 3.4. Comparison of One- and Two-Dimensional Heat-Transfer Performance For Copper Tube With e = 1.0 mm and t = 1.0 mm

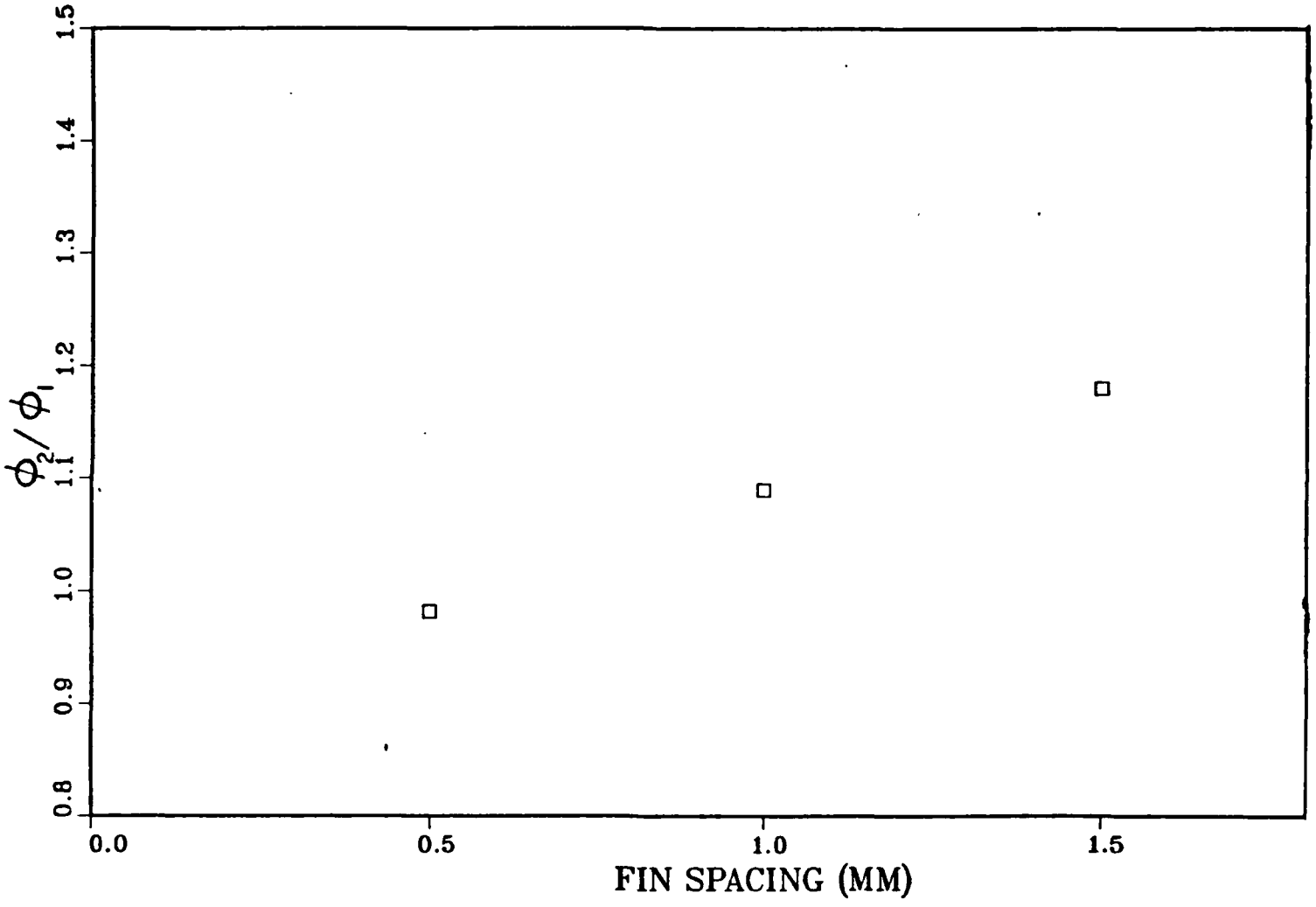

Figure 3.5. Comparison of One- and Two-Dimensional Heat-Transfer Performance For Copper-Nickel Tube With e = 1.0 mm and t = 1.0 mm

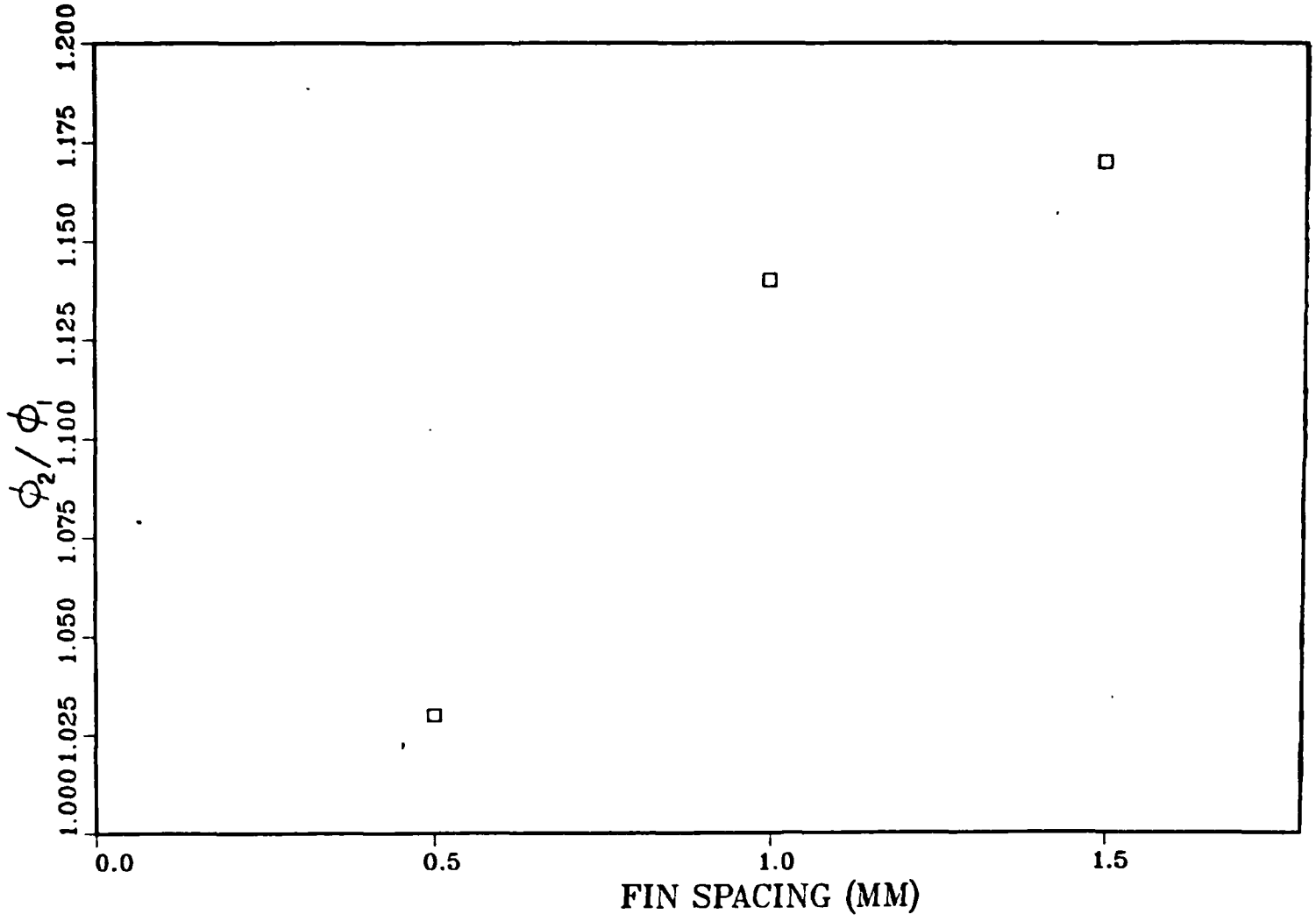

Figure 3.6. Comparison of One- and Two-Dimensional Heat-Transfer Performance For Stainless Steel Tube With e = 1.0 mm and t = 1.0 mm

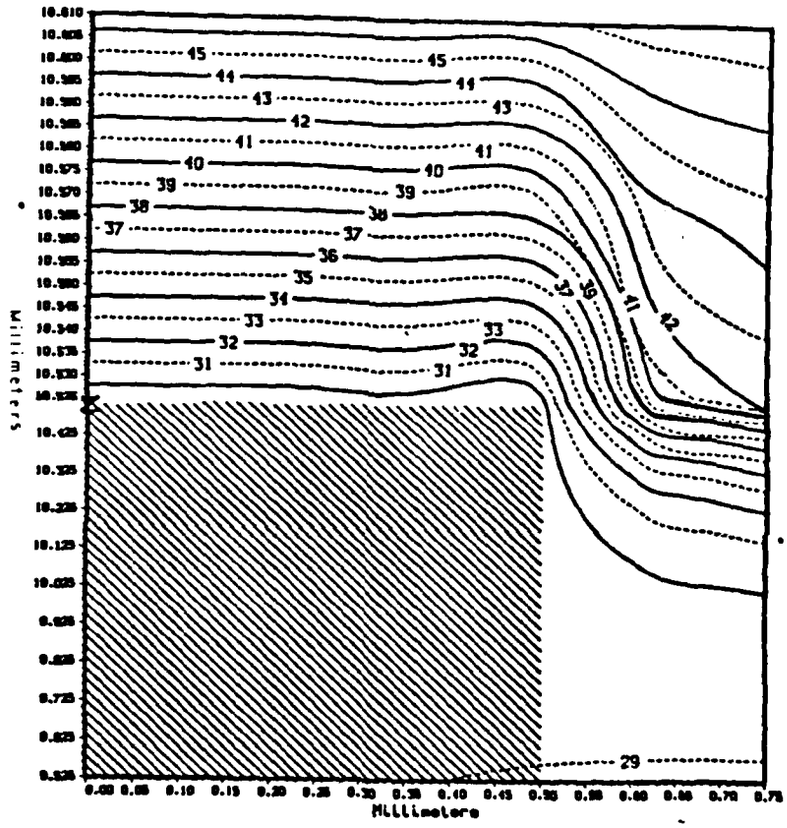

Figure 3.7. Isotherm Plot For Finned Copper Tube (Fin and Condensate Regions)

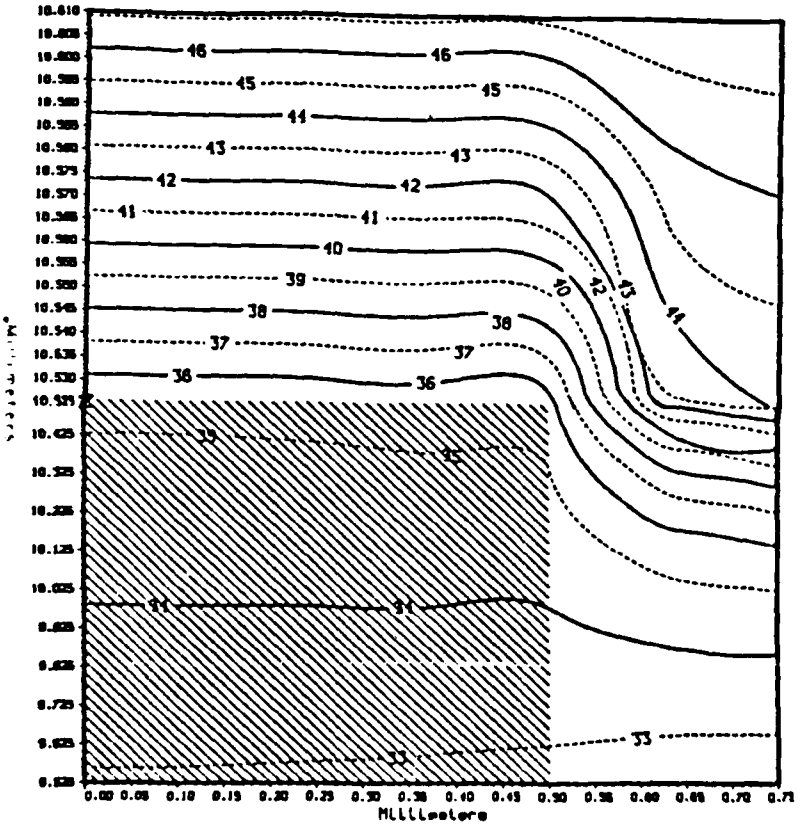

Figure 3.8. Isotherm Plot For Finned Copper-Nickel Tube (Fin and Condensate Regions)

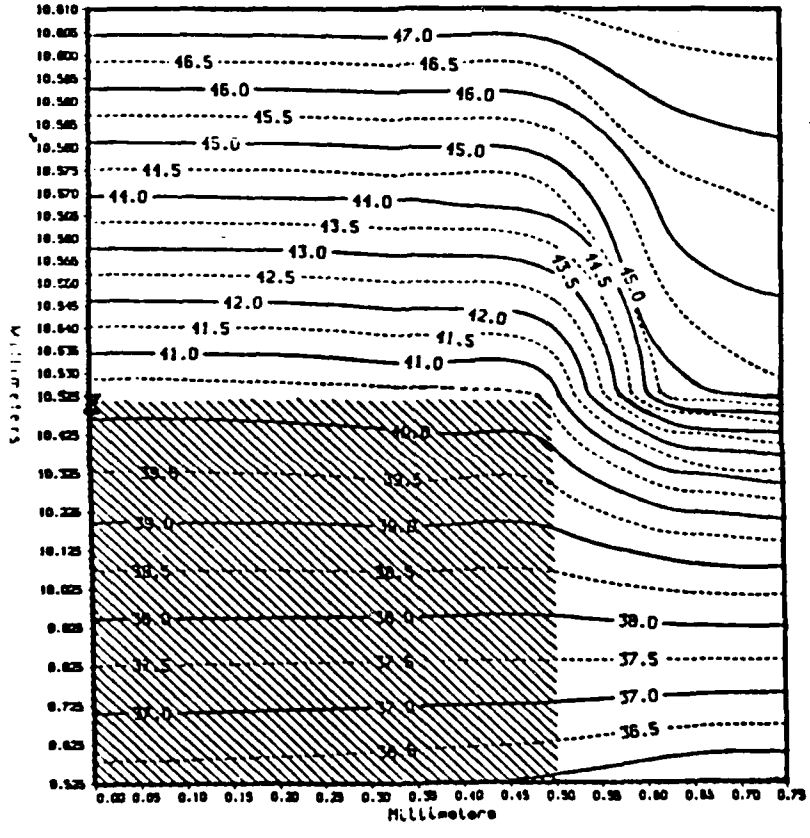

Figure 3.9. Isotherm Plot For Finned Stainless Steel Tube (Fin and Condensate Regions)

fin spacing is increased, the effect of the fin side surface is less pronounced since the poor conductivity of the condensate inhibits axial heat flow in the region near the fin space centerline. This results in a more closer agreement between the one-dimensional model and the two-dimensional version.

This conclusion can be further justified by comparing the Q21 ratios for each tube-metal conductivity. The two-dimensional effect at the fin tip is decreased as the thermal conductivity of the fin material decreases. This does not mean, however, that there is no two-dimensional effect for the cases with low tube-metal conductivity. As in the case of copper, the two-dimensional effect tends to inhibit the heat flow into the fin. For the cases of low metal thermal conductivity, there is a less pronounced two-dimensional effect at the fin tip, but there is a significant two-dimensional heat flow into the lower portion of the fin side surface near the tube wall. For this reason, the one-dimensional model tends to underpredict the two-dimensional model.

As seen in all the cases for the copper-nickel and stainless-steel tube-metal (except the copper-nickel case with 0.5 mm fin spacing), all Q21 ratios are greater than unity. For the copper-nickel case of 0.5 mm spacing, the reduced spacing even with a lower metal conductivity of 45 W/m.K, tends to produce a two-dimensional effect at the upper fin tip.

2. Effects of Fin Width

The results of the variation of heat flux with fin width as a parameter indicate that fin width plays an important

role in the overall heat-transfer mechanism. The two cases for each tube-metal thermal conductivity investigated were fin widths of 0.5 and 0.25 mm respectively with fin spacing held constant at 0.5 mm. For each case of tube-metal thermal conductivity, the fin width of 0.5 mm displayed one of the highest heat fluxes, being second only to the case of the 1.0 mm fin width with 0.5 mm fin spacing. The only significant two-dimensional fin tip effect can only be observed in the case of the copper tube-metal with a fin width of 0.5 mm.

The same reasoning as in the previous section can be applied in this case. Because the fin tip width has been reduced, the total amount of heat transferred into the tip region is also reduced and the two-dimensional fin tip choking effect has less influence. This concurs with the computed Q21 ratio of 1.04. By reducing the fin width further in each case to 0.25 mm, each of the resultant heat fluxes is less than the cases with 0.5 mm fin width. For each case of the 0.25 mm fin width the Q21 ratio approached 1.3, signifying the comparatively large two-dimensional heat flow into the lower fin side surface.

IV. CONCLUSIONS AND RECOMMENDATIONS

A. CONCLUSIONS

1. The two-dimensional numerical model of a horizontal finned tube fully flooded with steam condensate developed is a useful tool in the study of the relationship between one- and two-dimensional heat-transfer effects.

2. Two-dimensional heat transfer effects play a major role in the overall heat transfer mechanism in the case of an externally finned tube fully flooded with steam condensate. It has been determined that for cases of high tube-metal conductivity, such as the case of copper, the one-dimensional model can overpredict the results of the two-dimensional model by as much as 13%, while variation in the fin width or spacing can result in the one-dimensional model underpredicting the two-dimensional result by as much as twenty-two percent.

3. Fin width and fin spacing control the magnitude of the two-dimensional effect present and the resulting heat-transfer performance. An increasing fin width to fin spacing ratio will correspond to an increase in the heat-transfer performance.

4. The one-dimensional model in cases of high tube-metal thermal conductivity exhibiting a fin width to spacing ratio of greater than unity will overpredict the heat flux predictions of the two-dimensional model.

5. Decreasing the tube-metal thermal conductivity results in a degraded heat-transfer performance.

6. The two-dimensional fin-tip choking effect is minimal in low thermal conductivity tube-metals while the two-dimensional heat transfer into the fin lower side surface is far more pronounced.

B. RECOMMENDATIONS

1. Use the two-dimensional model computed enhancement ratios for the various cases to estimate a steam-side heat-transfer coefficient and compare with those methods currently being used.

2. Using the model builder TVIN and thermal analyzer TVSSI, conduct a more in-depth study of the effects of variation of fin width, height and spacing on the overall heat-transfer performance.

3. Revise the two-dimensional model to include convection effects in the retained condensate region.

APPENDIX A

TVIN COMPUTER GENERATED INPUT ANALYZER PROGRAM

```
CCCCCCCCCCCCCCCCCCCCCCCCCCCCCCCCCCCCCCCCCCCCCCCCCCCCCCCCCCCCCCCCCCCCCCC
C                        PROGRAM TVIN                                   C
C            PROGRAM TVIN IS DESIGNED TO ACCEPT VARIABLE                C
C            DIMENSIONS AND INPJT PARAMTERS TO CREATE                   C
C            AN OUTPUT DATA FILE OF INTER_NODE CONNECTIONS              C
C            AND CONDUCTANCE TERMS.  BY ADJUSTING THE                   C
C            PRINT STATEMENT, THE OUTPUT WILL EITHER                    C
C            REPRESENT A ONE OR TWO-DIMENSIONAL MODEL.                  C
C                                                                       C
CCCCCCCCCCCCCCCCCCCCCCCCCCCCCCCCCCCCCCCCCCCCCCCCCCCCCCCCCCCCCCCCCCCCCCC
C
C
      DIMENSION CK(300,4),T(300)
      INTEGER P(300,4),CO,N,X,ZW,ZW1,ZW2,ZW3,V1,V2,W,U,
      DOUBLE PRECISION CTHM,CTHL,HI,HS,RO,RI,A,B,C,D,
     *VAL4,VAL14,VAL6,VAL16,VAL8,VAL18,VAL5,VAL7,VAL10,
     *A2,A3,A4,A5,WINC1,WINC2,HINC1,HINC2,HINC3,ALINE,
     *TIN,TS,T,X1,X2,VAL2,VAL12,VAL20,A1,RADH,RADL,EL
      CHARACTER *79 TITLE
      CHARACTER *79 FNAME
C
      DATA IOT,IN,IPR,IWR/6,5,4,8/
C
      OPEN(IPR,FILE='PRN',STATUS='NEW',FORM='FORMATTED',
     *IOSTAT=ICK)
      IF(ICK .NE. 0) WRITE(IOT,20)
C
 20   FORMAT('TROUBLE OPENING PRINTER OUTPUT FILE')
C
      WRITE(IOT,17)
 17   FORMAT(/' ENTER THE TITLE OF THIS STUDY, 79 ',
     * ' COLUMNS MAX.  THIS TITLE WILL APPEAR',/,' AT ',
     * ' THE TOP OF EVERY PRINTED PAGE OF OUTPUT:')
      READ(IN,18) TITLE
 18   FORMAT(A79)
C
      WRITE(IOT,1)
  1   FORMAT(/' ENTER INNER RADIUS OF TUBE:')
      READ(IN,2) RI
  2   FORMAT(BN,F10.5)
C
      WRITE(IOT,3)
  3   FORMAT(/' ENTER OUTER RADIUS OF TUBE:')
      READ(IN,2) RO
C
      WRITE(IOT,4)
  4   FORMAT(/' ENTER DISTANCE FROM OUTER EDGE OF ',
     * 'FIN TO LIQUID SURFACE:')
      READ(IN,2) A
C
      WRITE(IOT,5)
  5   FORMAT(/' ENTER HEIGHT OF FIN')
      READ(IN,2) B
C
      WRITE(IOT,6)
  6   FORMAT(/' ENTER DISTANCE BETWEEN FINS')
      READ(IN,2) C
```

```
C
      WRITE(IOT,7)
    7 FORMAT(/' ENTER WIDTH OF FIN')
      READ(IN,2) D
C
      WRITE(IOT,8)
    8 FORMAT(/' ENTER HEAT TRANSFER COEFFICIENT OF ',
     *' TUBE INNER SURFACE:')
      READ(IN,2) HI
C
      WRITE(IOT,9)
    9 FORMAT(/' ENTER HEAT TRANSFER COEFFICIENT OF ',
     * 'OUTER LIQUID SURFACE:')
      READ(IN,2) HS
C
      WRITE(IOT,10)
   10 FORMAT(/' ENTER THERMAL CONDUCTIVITY OF FINS AND ',
     *' TUBE:')
      READ(IN,2) CTHM
C
      WRITE(IOT,11)
   11 FORMAT(/' ENTER THERMAL CONDUCTIVITY OF FLUID ' ,
     * ' SURROUNDING TUBE AND FINS:')
      READ(IN,2) CTHL
C
      WRITE(IOT,12)
   12 FORMAT(/' ENTER TEMPERATURE OF FLUID INSIDE TUBE:')
      READ(IN,2) TIN
C
      WRITE(IOT,13)
   13 FORMAT(/' ENTER TEMPERATURE EXTERNAL TO ',
     *' SURROUNDING FLUID:')
      READ(IN,2) TS
      WRITE(IOT,14)
   14 FORMAT(/' ENTER THE NUMBER OF COLUMNS DESIRED ',
     *' FOR YOUR MODEL: ')
      READ(IN,15) N
   15 FORMAT(BN,I2)

      WRITE(IOT,16)
   16 FORMAT(/' ENTER THE NUMBER OF ROWS DESIRED FOR ',
     *' THE TUBE:')
      READ(IN,15)U
      WRITE(IOT,99)
   99 FORMAT(/' ENTER THE NUMBER OF COLUMNS DESIRED FOR ',
     *' THE FIN: ')
      READ(IN,15)ZW
C
      CO=INT(300.0/FLOAT(N))
C   INITIALIZE THE P AND CK ARRAYS
C
      DO 25 I=1,CO*N
      DO 25 J=1,4
      P(I,J)=0
      CK(I,J)=0.0
25    CONTINUE
C
C   VALUES COMMON TO ALL RUNS
C
      L21=CO*N
      L22=2
      L23=0
```

```
      L24=0
      L25=0
      L26=0
      L27=0
      L28=0
C
      L31=300
      L32=50
      L33=6
      L34=2
      L35=4
      L36=6
C
      FL41=.01
      FL42=.66667
      IL43=12
      FL44=.8
      FL45=100.
C
      LINT1=0
      LINT2=0
      LINT3=0
C
C     COMPUTE INTERNODE CONNECTIONS
C
      DO 55 I=1,CO*N
      X=N*(CO-1)+1
      IF(AMOD(FLOAT(I-1),FLOAT(N)).EQ.0) GO TO 30
      IF(AMOD(FLOAT(I),FLOAT(N)).EQ.0) GO TO 40
      IF(I.LE.N) GO TO 42
      IF(I.GE.X) GO TO 48
C
C
      P(I,1)=(I-N)*10+1
      P(I,2)=(I-1)*10+1
      P(I,3)=(I+1)*10+1
      P(I,4)=(I+N)*10+1
      GO TO 55
C
C
30    IF(I.LE.N) GO TO 45
      IF(I.GE.X) GO TO 49
      P(I,2)=(I+1)*10+1
35    P(I,1)=(I-N)*10+1
      P(I,3)=(I+N)*10+1
      GO TO 55
C
C
40    IF(I.GE.X) GO TO 51
      IF(I.LE.N) GO TO 47
      P(I,2)=(I-1)*10+1
      GO TO 35
C
C
42    P(I,1)=(I-1)*10+1
      P(I,2)=(I+1)*10+1
      P(I,3)=(I+N)*10+1
      P(I,4)=3014
      GO TO 55
C
C
45    P(I,1)=(I*20)+1
46    P(I,2)=(I+N)*10+1
      P(I,3)=3014
      GO TO 55
```

```
C
C
47      P(I,1)=(I-1)*10+1
        GO TO 46
C
C
48      P(I,1)=(I-N)*10+1
        P(I,2)=(I-1)*10+1
        P(I,3)=(I+1)*10+1
        P(I,4)=3024
        GO TO 55
C
C
49      P(I,2)=(I-1)*10+1
50      P(I,1)=(I-N)*10+1
        P(I,3)=3024
        GO TO 55
C
C
51      P(I,2)=(I-1)*10+1
        GO TO 50
C
C
55      CONTINUE
C
C       CALCULATE HEIGHT AND WIDTH INCREMENTS
C
C       ZW=INT(FLOAT(N)/3.0)
        ZW1=N-ZW-1
C       ZW2=INT((FLOAT(CO)-10.0)/2.0)
        ZW2=2
        ZW3=CO-(U+1)-ZW2
        WINC1=D/FLOAT(ZW)
        WINC2=C/FLOAT(ZW1)
        HINC1=(RO-RI)/FLOAT(U)
        HINC2=B/FLOAT(ZW3)
        HINC3=A/FLOAT(ZW2)
        EL=(WINC1+WINC2)/2.0
C
C       COMPUTE THE RADIUS OF EACH ROW OF NODES
C
        DO 1000 I=1,CO
        IF(I.GT.1) GO TO 100
        RADH=RI+0.5*HINC1
        RADL=RI
        GO TO 150
C
100     IF(I.GE.(U+1)) GO TO 105
        RADH=RI+(FLOAT(I)-0.5)*HINC1
        RADL=RI+(FLOAT(I)-1.5)*HINC1
        GO TO 150
C
105     IF(I.NE.(U+1)) GO TO 110
        RADH=RO+HINC2/2.0
        RADL=RI+(FLOAT(I)-1.5)*HINC1
        GO TO 150
C
110     IF(I.GE.(11+ZW3)) GO TO 115
        RADH=RO+(FLOAT(I)-(FLOAT(U)+0.5))*HINC2
        RADL=RO+(FLOAT(I)-(FLOAT(U)+1.5))*HINC2
        GO TO 150
C
115     IF(I.NE.(U+1+ZW3)) GO TO 120
        RADH=RO+B+HINC3/2.0
        RADL=RO+B-HINC2/2.0
```

```
      GO TO 150
C
120   IF(I.EQ.CO) GO TO 125
      RADH=RO+B+(FLOAT(I)-(FLOAT(U)+0.5)-FLOAT(ZW3))*HINC3
      RADL=RO+B+(FLOAT(I)-(FLOAT(U)+1.5)-FLOAT(ZW3))*HINC3
      GO TO 150
C
125   RADH=RO+B+A
      RADL=RO+B+A-HINC3/2.0
C
CC
CC
150   ALINE=RADH**2-RADL**2
C
C     COMPUTE INTER-NODE CONDUCTANCE VALJES
CC
CC
185   IF(I.GT.1) GO TO 187
      HTC=HI
      RD=RI
      GO TO 189
187   IF(I.NE.CO) GO TO 190
      HTC=HS
      RD=RO+A+B
189   A1=HTC*WINC1*RD/2.0
      A2=A1*2.0
      A3=A2*EL/WINC1
      A4=HTC*WINC2*RD
      A5=A4/2.0
C
CC
190   IF(I.GE.(U+2)) GO TO 200
C
      VAL4=RADL*WINC1*CTHM/HINC1
      GO TO 300
200   IF(I.GE.((U+2)+ZW3)) GO TO 250
      VAL4=RADL*WINC1*CTHM/HINC2
      GO TO 300
250   VAL4=CTHL*RADL*WINC1/HINC3
300   VAL2=VAL4/2.0
CC
CCC
C
      IF(I.GE.(U+1)) GO TO 310
      VAL14=CTHM*RADH*WINC1/HINC1
      GO TO 400
310   IF(I.LE.(U+ZW3)) GO TO 350
      VAL14=CTHL*RADH*WINC1/HINC3
      GO TO 400
350   VAL14=CTHM*RADH*WINC1/HINC2
400   VAL12=VAL14/2.0
C
CC
C
      IF(I.GE.(U+2)) GO TO 410
      VAL6=CTHM*RADL*EL/HINC1
      GO TO 500
410   IF(I.GE.((U+2)+ZW3)) GO TO 450
      VAL6=((CTHM*WINC1+CTHL*WINC2)*RADL)/(2.0*HINC2)
      GO TO 500
450   VAL6=CTHL*RADL*EL/HINC3
C
CC
C
```

```
500   IF(I.GE.(U+1)) GO TO 610
      VAL16=CTHM*EL*RADH/HINC1
      GO TO 650
610   IF(I.LE.(U+ZW3)) GO TO 620
      VAL16=CTHL*EL*RADH/HINC3
      GO TO 650
620   VAL16=((CTHM*WINC1+CTHL*WINC2)*RADH)/(2.0*HINC2)
C
C
C
650   IF(I.GE.(U+2)) GO TO 670
      VAL8=RADL*WINC2*CTHM/HINC1
      GO TO 700
670   IF(I.GE.((U+2)+ZW3)) GO TO 680
      VAL8=CTHL*RADL*WINC2/HINC2
      GO TO 700
680   VAL8=CTHL*RADL*WINC2/HINC3
700   VAL10=VAL8/2.0
C
C
C
      IF(I.GE.(U+1)) GO TO 730
      VAL18=CTHM*RADH*WINC2/HINC1
      GO TO 750
730   IF(I.LE.(U+ZW3)) GO TO 740
      VAL18=CTHL*RADH*WINC2/HINC3
      GO TO 750
740   VAL18=CTHL*RADH*WINC2/HINC2
750   VAL20=VAL18/2.0
C
C
C
      IF(I.NE.((U+1)+ZW3)) GO TO 760
      VAL5=(CTHL*(RADH**2-(RO+B)**2)+CTHM*((RO+B)
     ***2-RADL**2))/(2.0*WINC1)
      GO TO 800
760   IF(I.GT.((U+1)+ZW3)) GO TO 770
      VAL5=CTHM*ALINE/(2.0*WINC1)
      GO TO 800
770   VAL5=CTHL*ALINE/(2.0*WINC1)
C
C
C
800   IF(I.GE.(U+1)) GO TO 810
      VAL7=CTHM*ALINE/(2.0*WINC2)
      GO TO 845
810   IF(I.NE.(U+1)) GO TO 820
      VAL7=(CTHL*(RADH**2-RO**2)+CTHM*(RO**2-RADL**2))
     */(2.0*WINC2)
      GO TO 845
820   VAL7=CTHL*ALINE/(2.0*WINC2)
C
C     COUPLE CONDUCTANCE VALUES TO CONNECTION TERMS
C
845   IF(I.EQ.1) GO TO 905
      IF(I.EQ.CO) GO TO 912
      Q=N*(I-1)
850   DO 900 J=Q+1,Q+N
C
C
860   IF(J.EQ.(Q+1)) GO TO 875
      IF(J.LT.(Q+ZW+1)) GO TO 880
      IF(J.EQ.(Q+ZW+1)) GO TO 885
      IF(J.NE.(Q+N)) GO TO 890
C
```

```
C
      CK(J,1)=VAL10
      CK(J,2)=VAL7
      CK(J,3)=VAL20
      GO TO 900
C
C
880   CK(J,1)=VAL4
      CK(J,2)=VAL5
      CK(J,3)=VAL5
      CK(J,4)=VAL14
      GO TO 900
C
C
885   CK(J,1)=VAL6
      CK(J,2)=VAL5
      CK(J,3)=VAL7
      CK(J,4)=VAL16
      GO TO 900
C
C
890   CK(J,1)=VAL8
      CK(J,2)=VAL7
      CK(J,3)=VAL7
      CK(J,4)=VAL18
      GO TO 900
C
C
875   CK(J,1)=VAL2
      CK(J,2)=VAL5
      CK(J,3)=VAL12
C
900   CONTINUE
901   GO TO 1000
C
C
905   DO 910 J=1,N
      IF(J.GT.1) GO TO 906
      CK(J,1)=VAL5
      CK(J,2)=VAL12
      CK(J,3)=A1
      GO TO 910
C
C
906   IF(J.GE.ZW+1) GO TO 907
      CK(J,1)=VAL5
      CK(J,2)=VAL5
      CK(J,3)=VAL14
      CK(J,4)=A2
      GO TO 910
C
C
907   IF(J.NE.(ZW+1)) GO TO 908
      CK(J,1)=VAL5
      CK(J,2)=VAL7
      CK(J,3)=VAL16
      CK(J,4)=A3
      GO TO 910
C
C
908   IF(J.EQ.N) GO TO 909
      CK(J,1)=VAL7
      CK(J,2)=VAL7
      CK(J,3)=VAL18
      CK(J,4)=A4
```

```
      GO TO 910
C
C
909   CK(J,1)=VAL7
      CK(J,2)=VAL20
      CK(J,3)=A5
C
910   CONTINUE
C
C
911   GO TO 1000
C
C
912   Q=(CO-1)*N
      DO 917 J=Q+1,Q+N
      IF(J.GT.(Q+1)) GO TO 913
      CK(J,1)=VAL2
      CK(J,2)=VAL5
      CK(J,3)=A1
      GO TO 917
C
C
913   IF(J.GE.(ZW+Q+1)) GO TO 914
      CK(J,1)=VAL4
      CK(J,2)=VAL5
      CK(J,3)=VAL5
      CK(J,4)=A2
      GO TO 917
C
C
914   IF(J.NE.(ZW+Q+1)) GO TO 915
      CK(J,1)=VAL6
      CK(J,2)=VAL5
      CK(J,3)=VAL7
      CK(J,4)=A3
      GO TO 917
C
C
915   IF(J.EQ.(Q+N)) GO TO 916
      CK(J,1)=VAL8
      CK(J,2)=VAL7
      CK(J,3)=VAL7
      CK(J,4)=A4
      GO TO 917
C
C
916   CK(J,1)=VAL10
      CK(J,2)=VAL7
      CK(J,3)=A5
917   CONTINUE
1000  CONTINUE
C
C
C   END OF CONDUCTANCE CALCULATIONS
      WRITE(IOT,922)
922   FORMAT(/,' ENTER NAME OF INPUT FILE':)
      READ(IN,923)FNAME
923   FORMAT(A12)
C
C
C   CREATE DATA FILE FOR TVSSI
C
      OPEN(IWR,FILE=FNAME,STATUS='NEW',FORM='FORMATTED',
     *IOSTAT=ICK)
C
```

```
C
      WRITE(IOT,925)
925   FORMAT(/' WRITING FILE TVSSI')
C
      WRITE(IOT,926)CO*N,N,CO,ZW2
926   FORMAT(/' THIS ',I3,' NODE MODEL HAS ',I2,' ROWS '
     *' AND ',I2,' COLUMNS.  THERE ARE ',I2,' ROWS')
      WRITE(IOT,927)ZW3
927   FORMAT(' IN THE CONDESATE LAYER AND ',I2,' ROWS ',
     *' IN THE FIN. THE FIN CONTAINS')
      WRITE(IOT,928)ZW
928   FORMAT(I2,' COLUMNS. ')
C
C   WRITE STATEMENTS
C
      WRITE(IWR,940) TITLE
      WRITE(IWR,944)L21,L22,L23,L24,L25,L26,L27,L28
      WRITE(IWR,950)LINT1,LINT2,LINT3
      WRITE(IWR,946)L31,L32,L33,L34,L35,L36
      WRITE(IWR,947)FL41,FL42,IL43,FL44,FL45
      WRITE(IWR,943)TI,TS
C
      DO 1100 I=1,CO*N
      IF (P(I,4).EQ.0) GO TO 1011
      IF(CK(I,1).GE.100.0.OR.CK(I,2).GE.100.0)GO TO 1005
      IF(CK(I,3).GE.100.0.OR.CK(I,4).GE.100.0)GO TO 1005
      WRITE(IWR,948)P(I,1),P(I,2),P(I,3),P(I,4)
      WRITE(IWR,960)CK(I,1),CK(I,2),CK(I,3),CK(I,4)
      GO TO 1100
1005  WRITE(IWR,948)P(I,1),P(I,2),P(I,3),P(I,4)
      WRITE(IWR,942)CK(I,1),CK(I,2),CK(I,3),CK(I,4)
      GO TO 1100
1011  IF(CK(I,1).GE.100.0.OR.CK(I,2).GE.100.0) GO TO 1015
      IF(CK(I,3).GE.100.0) GO TO 1015
      WRITE(IWR,945)P(I,1),P(I,2),P(I,3)
      WRITE(IWR,949)CK(I,1),CK(I,2),CK(I,3)
      GO TO 1100
1015  WRITE(IWR,945)P(I,1),P(I,2),P(I,3)
      WRITE(IWR,980)CK(I,1),CK(I,2),CK(I,3)
C
1100  CONTINUE
C
C   FORMAT STATEMENTS
C
940   FORMAT(1X,A79)
941   FORMAT(6F8.5)
942   FORMAT(4F8.4)
943   FORMAT(2F8.0)
C
944   FORMAT(9I4)
945   FORMAT(9I8)
946   FORMAT(9I4)
947   FORMAT(F8.3,F8.5,I8,2F8.1)
948   FORMAT(9I8)
949   FORMAT(F8.6,F8.5,F8.6)
950   FORMAT(9I4)
960   FORMAT(F8.6,2F8.5,F8.6)
980   FORMAT(3F8.4)
C
C
      CLOSE(IWR,IOSTAT=ICK)
      IF(ICK .NE. 0) WRITE(IOT,921)EEX
921   FORMAT('TROUBLE CLOSING PRINTER OUTPUT FILE')
C
C
```

```
STOP
END
```

APPENDIX B

Q1 COMPUTER GENERATED MODEL VERIFIER PROGRAM

```
CCCCCCCCCCCCCCCCCCCCCCCCCCCCCCCCCCCCCCCCCCCCCCCCCCCCCCCCCCCCCCCCCCCC
C                          PROGRAM Q1                                  C
C            PROGRAM Q1 IS DESIGNED TO ACCEPT VARIABLE                 C
C            DIMENSIONS, INPUT A DATA FILE OF NODE                     C
C            TEMPERATURES GENERATED BY TVSSI AND CREATE                C
C            AN OUPUT FILE OF HEAT FLOW VALUES ACROSS                  C
C            1) VAPOR CONDENSATE INTERFACE, 2) FIN AND                 C
C      TUBE OUTER PERIMETER, AND TUBE INNER WALL                       C
C                                                                      C
CCCCCCCCCCCCCCCCCCCCCCCCCCCCCCCCCCCCCCCCCCCCCCCCCCCCCCCCCCCCCCCCCCCC
C
C
      DIMENSION CK(300,4),T(300)
      INTEGER P(300,4),CO,N,X,ZW,ZW1,ZW2,ZW3,V1,V2,W,U,
      DOUBLE PRECISION CTHM,CTHL,HI,HS,RO,RI,A,B,C,D,
     *VAL4,VAL14,VAL6,VAL16,VAL8,VAL18,VAL5,VAL7,VAL10,
     *A2,A3,A4,A5,WINC1,WINC2,HINC1,HINC2,HINC3,ALINE,
     *TIN,TS,T,X1,X2,VAL2,VAL12,VAL20,A1,RADH,RADL,EL
      CHARACTER *79 TITLE
      CHARACTER *79 FNAME
C
      DATA IOT,IN,IPR,IWR/6,5,4,8/
C
      OPEN(IPR,FILE='PRN',STATUS='NEW',FORM='FORMATTED',
     *IOSTAT=ICK)
      IF(ICK .NE. 0) WRITE(IOT,20)
C
 20   FORMAT('TROUBLE OPENING PRINTER OUTPUT FILE')
C
      WRITE(IOT,17)
 17   FORMAT(/' ENTER THE TITLE OF THIS STUDY, 79 ',
     * ' COLUMNS MAX.  THIS TITLE WILL APPEAR',/,' AT',
     * ' THE TOP OF EVERY PRINTED PAGE OF OUTPUT:')
      READ(IN,18) TITLE
 18   FORMAT(A79)
C
      WRITE(IOT,1)
  1   FORMAT(/' ENTER INNER RADIUS OF TUBE:')
      READ(IN,2) RI
  2   FORMAT(BN,F10.5)
C
      WRITE(IOT,3)
  3   FORMAT(/' ENTER OUTER RADIUS OF TUBE:')
      READ(IN,2) RO
C
      WRITE(IOT,4)
  4   FORMAT(/' ENTER DISTANCE FROM OUTER EDGE OF ',
     * 'FIN TO LIQUID SURFACE:')
      READ(IN,2) A
C
      WRITE(IOT,5)
  5   FORMAT(/' ENTER HEIGHT OF FIN')
      READ(IN,2) B
C
      WRITE(IOT,6)
  6   FORMAT(/' ENTER DISTANCE BETWEEN FINS')
      READ(IN,2) C
```

```
C
      WRITE(IOT,7)
    7 FORMAT(/' ENTER WIDTH OF FIN')
      READ(IN,2) D
C
      WRITE(IOT,8)
    8 FORMAT(/' ENTER HEAT TRANSFER COEFFICIENT OF ',
     *' TUBE INNER SURFACE:')
      READ(IN,2) HI
C
      WRITE(IOT,9)
    9 FORMAT(/' ENTER HEAT TRANSFER COEFFICIENT OF ',
     * 'OUTER LIQUID SURFACE:')
      READ(IN,2) HS
C
      WRITE(IOT,10)
   10 FORMAT(/' ENTER THERMAL CONDUCTIVITY OF FINS AND ',
     *' TUBE:')
      READ(IN,2) CTHM
C
      WRITE(IOT,11)
   11 FORMAT(/' ENTER THERMAL CONDUCTIVITY OF FLUID ' ,
     * ' SURROUNDING TUBE AND FINS:')
      READ(IN,2) CTHL
C
      WRITE(IOT,12)
   12 FORMAT(/' ENTER TEMPERATURE OF FLUID INSIDE TUBE:')
      READ(IN,2) TIN
C
      WRITE(IOT,13)
   13 FORMAT(/' ENTER TEMPERATURE EXTERNAL TO ',
     *' SURROUNDING FLUID:')
      READ(IN,2) TS
      WRITE(IOT,14)
   14 FORMAT(/' ENTER THE NUMBER OF COLUMNS DESIRED ',
     *' FOR YOUR MODEL: ')
      READ(IN,15) N
   15 FORMAT(BN,I2)

      WRITE(IOT,16)
   16 FORMAT(/' ENTER THE NUMBER OF ROWS DESIRED FOR ',
     *' THE TUBE:')
      READ(IN,15)U
      WRITE(IOT,99)
   99 FORMAT(/' ENTER THE NUMBER OF COLUMNS DESIRED FOR ',
     *' THE FIN: ')
      READ(IN,15)ZW
C
      CO=INT(300.0/FLOAT(N))
C   INITIALIZE THE P AND CK ARRAYS
C
      DO 25 I=1,CO*N
      DO 25 J=1,4
      P(I,J)=0
      CK(I,J)=0.0
25    CONTINUE
C
C   VALUES COMMON TO ALL RUNS
C
      L21=CO*N
      L22=2
      L23=0
```

```
      L24=0
      L25=0
      L26=0
      L27=0
      L28=0
C
      L31=300
      L32=50
      L33=6
      L34=2
      L35=4
      L36=6
C
      FL41=.01
      FL42=.66667
      IL43=12
      FL44=.8
      FL45=100.
C
      LINT1=0
      LINT2=0
      LINT3=0
C
C     COMPUTE INTERNODE CONNECTIONS
C
      DO 55 I=1,CC*N
      X=N*(CO-1)+1
      IF(AMOD(FLOAT(I-1),FLOAT(N)).EQ.0) GO TO 30
      IF(AMOD(FLOAT(I),FLOAT(N)).EQ.0) GO TO 40
      IF(I.LE.N) GO TO 42
      IF(I.GE.X) GO TO 48
C
C
      P(I,1)=(I-N)*10+1
      P(I,2)=(I-1)*10+1
      P(I,3)=(I+1)*10+1
      P(I,4)=(I+N)*10+1
      GO TO 55
C
C
30    IF(I.LE.N) GO TO 45
      IF(I.GE.X) GO TO 49
      P(I,2)=(I+1)*10+1
35    P(I,1)=(I-N)*10+1
      P(I,3)=(I+N)*10+1
      GO TO 55
C
C
40    IF(I.GE.X) GO TO 51
      IF(I.LE.N) GO TO 47
      P(I,2)=(I-1)*10+1
      GO TO 35
C
C
42    P(I,1)=(I-1)*10+1
      P(I,2)=(I+1)*10+1
      P(I,3)=(I+N)*10+1
      P(I,4)=3014
      GO TO 55
C
C
45    P(I,1)=(I*20)+1
46    P(I,2)=(I+N)*10+1
      P(I,3)=3014
      GO TO 55
```

```
C
C
47      P(I,1)=(I-1)*10+1
        GO TO 46
C
C
48      P(I,1)=(I-N)*10+1
        P(I,2)=(I-1)*10+1
        P(I,3)=(I+1)*10+1
        P(I,4)=3024
        GO TO 55
C
C
49      P(I,2)=(I-1)*10+1
50      P(I,1)=(I-N)*10+1
        P(I,3)=3024
        GO TO 55
C
C
51      P(I,2)=(I-1)*10+1
        GO TO 50
C
C
55      CONTINUE
C
C       CALCULATE HEIGHT AND WIDTH INCREMENTS
C
C       ZW=INT(FLOAT(N)/3.0)
        ZW1=N-ZW-1
C       ZW2=INT((FLOAT(CO)-10.0)/2.0)
        ZW2=2
        ZW3=CO-(U+1)-ZW2
        WINC1=D/FLOAT(ZW)
        WINC2=C/FLOAT(ZW1)
        HINC1=(RO-RI)/FLOAT(U)
        HINC2=B/FLOAT(ZW3)
        HINC3=A/FLOAT(ZW2)
        EL=(WINC1+WINC2)/2.0
C
C       COMPUTE THE RADIUS OF EACH ROW OF NODES
C
        DO 1000 I=1,CO
        IF(I.GT.1) GO TO 100
        RADH=RI+0.5*HINC1
        RADL=RI
        GO TO 150
C
100     IF(I.GE.(U+1)) GO TO 105
        RADH=RI+(FLOAT(I)-0.5)*HINC1
        RADL=RI+(FLOAT(I)-1.5)*HINC1
        GO TO 150
C
105     IF(I.NE.(U+1)) GO TO 110
        RADH=RO+HINC2/2.0
        RADL=RI+(FLOAT(I)-1.5)*HINC1
        GO TO 150
C
110     IF(I.GE.(11+ZW3)) GO TO 115
        RADH=RO+(FLOAT(I)-(FLOAT(U)+0.5))*HINC2
        RADL=RO+(FLOAT(I)-(FLOAT(U)+1.5))*HINC2
        GO TO 150
C
115     IF(I.NE.(U+1+ZW3)) GO TO 120
        RADH=RO+B+HINC3/2.0
        RADL=RO+B-HINC2/2.0
```

```
      GO TO 150
C
120   IF(I.EQ.CO) GO TO 125
      RADH=RO+B+(FLOAT(I)-(FLOAT(U)+0.5)-FLOAT(ZW3))*HINC3
      RADL=RO+B+(FLOAT(I)-(FLOAT(U)+1.5)-FLOAT(ZW3))*HINC3
      GO TO 150
C
125   RADH=RO+B+A
      RADL=RO+B+A-HINC3/2.0
C
CC
C
150   ALINE=RADH**2-RADL**2
C
C     COMPUTE INTER-NODE CONDUCTANCE VALUES
CC
C
185   IF(I.GT.1) GO TO 187
      HTC=HI
      RD=RI
      GO TO 189
187   IF(I.NE.CO) GO TO 190
      HTC=HS
      RD=RO+A+B
189   A1=HTC*WINC1*RD/2.0
      A2=A1*2.C
      A3=A2*EL/WINC1
      A4=HTC*WINC2*RD
      A5=A4/2.0
C
CC
190   IF(I.GE.(U+2)) GO TO 200
C
      VAL4=RADL*WINC1*CTHM/HINC1
      GO TO 300
200   IF(I.GE.((U+2)+ZW3)) GO TO 250
      VAL4=RADL*WINC1*CTHM/HINC2
      GO TO 300
250   VAL4=CTHL*RADL*WINC1/HINC3
300   VAL2=VAL4/2.0
C
CC
CC
C
      IF(I.GE.(U+1)) GO TO 310
      VAL14=CTHM*RADH*WINC1/HINC1
      GO TO 400
310   IF(I.LE.(U+ZW3)) GO TO 350
      VAL14=CTHL*RADH*WINC1/HINC3
      GO TO 400
350   VAL14=CTHM*RADH*WINC1/HINC2
400   VAL12=VAL14/2.0
C
CC
C
      IF(I.GE.(U+2)) GO TO 410
      VAL6=CTHM*RADL*EL/HINC1
      GO TO 500
410   IF(I.GE.((U+2)+ZW3)) GO TO 450
      VAL6=((CTHM*WINC1+CTHL*WINC2)*RADL)/(2.0*HINC2)
      GO TO 500
450   VAL6=CTHL*RADL*EL/HINC3
C
CC
C
```

```
500   IF(I.GE.(U+1)) GO TO 610
      VAL16=CTHM*EL*RADH/HINC1
      GO TO 650
610   IF(I.LE.(U+ZW3)) GO TO 620
      VAL16=CTHL*EL*RADH/HINC3
      GO TO 650
620   VAL16=((CTHM*WINC1+CTHL*WINC2)*RADH)/(2.0*HINC2)
C
C
C
650   IF(I.GE.(U+2)) GO TO 670
      VAL8=RADL*WINC2*CTHM/HINC1
      GO TO 700
670   IF(I.GE.((U+2)+ZW3)) GO TO 680
      VAL8=CTHL*RADL*WINC2/HINC2
      GO TO 700
680   VAL8=CTHL*RADL*WINC2/HINC3
700   VAL10=VAL8/2.0
C
C
C
      IF(I.GE.(U+1)) GO TO 730
      VAL18=CTHM*RADH*WINC2/HINC1
      GO TO 750
730   IF(I.LE.(U+ZW3)) GO TO 740
      VAL18=CTHL*RADH*WINC2/HINC3
      GO TO 750
740   VAL18=CTHL*RADH*WINC2/HINC2
750   VAL20=VAL18/2.0
C
C
C
      IF(I.NE.((U+1)+ZW3)) GO TO 760
      VAL5=(CTHL*(RADH**2-(RO+B)**2)+CTHM*((RO+B)
     ***2-RADL**2))/(2.0*WINC1)
      GO TO 800
760   IF(I.GT.((U+1)+ZW3)) GO TO 770
      VAL5=CTHM*ALINE/(2.0*WINC1)
      GO TO 800
770   VAL5=CTHL*ALINE/(2.0*WINC1)
C
C
C
800   IF(I.GE.(U+1)) GO TO 810
      VAL7=CTHM*ALINE/(2.0*WINC2)
      GO TO 845
810   IF(I.NE.(U+1)) GO TO 820
      VAL7=(CTHL*(RADH**2-RO**2)+CTHM*(RO**2-RADL**2))
     */(2.0*WINC2)
      GO TO 845
820   VAL7=CTHL*ALINE/(2.0*WINC2)
C
C     COUPLE CONDUCTANCE VALUES TO CONNECTION TERMS
C
845   IF(I.EQ.1) GO TO 905
      IF(I.EQ.CO) GO TO 912
      Q=N*(I-1)
850   DO 900 J=Q+1,Q+N
C
C
860   IF(J.EQ.(Q+1)) GO TO 875
      IF(J.LT.(Q+ZW+1)) GO TO 880
      IF(J.EQ.(Q+ZW+1)) GO TO 885
      IF(J.NE.(Q+N)) GO TO 890
C
```

```
C
      CK(J,1)=VAL10
      CK(J,2)=VAL7
      CK(J,3)=VAL20
      GO TO 900
C
C
880   CK(J,1)=VAL4
      CK(J,2)=VAL5
      CK(J,3)=VAL5
      CK(J,4)=VAL14
      GO TO 900
C
C
885   CK(J,1)=VAL6
      CK(J,2)=VAL5
      CK(J,3)=VAL7
      CK(J,4)=VAL16
      GO TO 900
C
C
890   CK(J,1)=VAL8
      CK(J,2)=VAL7
      CK(J,3)=VAL7
      CK(J,4)=VAL18
      GO TO 900
C
C
875   CK(J,1)=VAL2
      CK(J,2)=VAL5
      CK(J,3)=VAL12
C
900   CONTINUE
901   GO TO 1000
C
C
905   DO 910 J=1,N
      IF(J.GT.1) GO TO 906
      CK(J,1)=VAL5
      CK(J,2)=VAL12
      CK(J,3)=A1
      GO TO 910
C
C
906   IF(J.GE.ZW+1) GO TO 907
      CK(J,1)=VAL5
      CK(J,2)=VAL5
      CK(J,3)=VAL14
      CK(J,4)=A2
      GO TO 910
C
C
907   IF(J.NE.(ZW+1)) GO TO 908
      CK(J,1)=VAL5
      CK(J,2)=VAL7
      CK(J,3)=VAL16
      CK(J,4)=A3
      GO TO 910
C
C
908   IF(J.EQ.N) GO TO 909
      CK(J,1)=VAL7
      CK(J,2)=VAL7
      CK(J,3)=VAL18
      CK(J,4)=A4
```

```
      GO TO 910
C
C
909   CK(J,1)=VAL7
      CK(J,2)=VAL20
      CK(J,3)=A5
C
910   CONTINUE
C
C
911   GO TO 1000
C
C
912   Q=(CO-1)*N
      DO 917 J=Q+1,Q+N
      IF(J.GT.(Q+1)) GO TO 913
      CK(J,1)=VAL2
      CK(J,2)=VAL5
      CK(J,3)=A1
      GO TO 917
C
C
913   IF(J.GE.(ZW+Q+1)) GO TO 914
      CK(J,1)=VAL4
      CK(J,2)=VAL5
      CK(J,3)=VAL5
      CK(J,4)=A2
      GO TO 917
C
C
914   IF(J.NE.(ZW+Q+1)) GO TO 915
      CK(J,1)=VAL6
      CK(J,2)=VAL5
      CK(J,3)=VAL7
      CK(J,4)=A3
      GO TO 917
C
C
915   IF(J.EQ.(Q+N)) GO TO 916
      CK(J,1)=VAL8
      CK(J,2)=VAL7
      CK(J,3)=VAL7
      CK(J,4)=A4
      GO TO 917
C
C
916   CK(J,1)=VAL10
      CK(J,2)=VAL7
      CK(J,3)=A5
917   CONTINUE
1000  CONTINUE
C
C
C   END OF CONDUCTANCE CALCULATIONS
      WRITE(IOT,922)
922   FORMAT(/,' ENTER NAME OF INPUT FILE':)
      READ(IN,923)FNAME
923   FORMAT(A12)
C
C
C   CREATE DATA FILE FOR TVSSI
C
      OPEN(IWR,FILE=FNAME,STATUS='NEW',FORM='FORMATTED',
     *IOSTAT=ICK)
C
```

```
C     READ IN NODE TEMPERATURES GENERATED BY TVSSI
C
C
      DO 924 J=1,25
      READ(16,1045)(T(I),I=((J-1)*12+1),J*12)
924   CONTINUE
C
      WRITE(IOT,925)
925   FORMAT(/' WRITING FILE TVSSI')
C
      WRITE(IOT,926)CO*N,CO,N,ZW2
926   FORMAT(/' THIS ',I3,' NODE MODEL HAS ',I2,' ROWS '
     *' AND ',I2,' COLUMNS.  THERE ARE ',I2,' ROWS')
      WRITE(IOT,927)ZW3
927   FORMAT(' IN THE CONDESATE LAYER AND ',I2,
     *' IN THE FIN.  THE FIN CONTAINS')
      WRITE(IOT,928)ZW
928   FORMAT(I2,' COLUMNS. ')
C
C     COMPUTE HEAT FLOW ACROSS DESIGNATED SURFACES
C
      QFL=0.0
      QFS=0.0
      QFU=0.0
      QU=0.0
      QO=0.0
C
C
      DO 2000 I=1,N
949   IF(I.GT.(N-ZW-1)) GO TO 955
      V1=(U+1)*N+1+ZW+I
      V2=(U*N)+1+ZW+I
      IF(V2.EQ.(U+1)*N) GO TO 950
      QFL=QFL+(T(V1)-T(V2))*CK(V2,4)
      GO TO 955
950   QFL=QFL+(T(V1)-T(V2))*CK(V2,3)
955   IF(I.GT.ZW3) GO TO 960
      W=N*(U+I)+2+ZW
      QFS=QFS+(T(W)-T(W-1))*CK(W,3)
960   IF(I.GT.(ZW+1)) GO TO 970
      X1=(U+ZW3)*N+I
      X2=(U+ZW3+1)*N+I
      IF(I.EQ.1) GO TO 965
      QFL=QFU+(T(X2)-T(X1))*CK(X1,4)
      WRITE(6,9000)QFU,T(X2),T(X1),CK(X1,4),X1,X2
      GO TO 970
965   QFU=QFU+(T(X2)-T(X1))*CK(X1,3)
      WRITE(6,9000)QFU,T(X2),T(X1),CK(X1,3),X1,X2
9000  FORMAT(1X,4F10.5,2I3)
970   IF(I.GT.1)GO TO 980
975   QO=QO+(T(I)-TIN)*CK(I,3)
      QU=QU+(TS-T(I+(N*(CO-1))))*CK((I+(N*(CO-1))),3)
      GO TO 2000
980   IF(I.EQ.N) GO TO 975
      QO=QO+(T(I)-TIN)*CK(I,4)
      QU=QU+(TS-T(I+(N*(CO-1))))*CK((I+(N*(CO-1))),4)
2000  CONTINUE
      QT1=QFU+QFS
      QTO=QT1+QFL
C     WRITE STATEMENTS
      WRITE(IWR,1030)
      WRITE(IWR,1031)RI,RO,B
      WRITE(IWR,1032)
      WRITE(IWR,1033) C,D,A
```

```
      WRITE(IWR,1034)
      WRITE(IWR,1035)TIN,TS
      WRITE(IWR,1036)
      WRITE(IWR,1037)CTHM,CTHL,HI,HS
      WRITE(IWR,1047)QFU
      WRITE(IWR,1048)QFS
      WRITE(IWR,1040)QTI
      WRITE(IWR,1041)QFL
      WRITE(IWR,1042)QTO
      WRITE(IWR,1043)QU
      WRITE(IWR,1044)QD
C
1030  FORMAT(/' PIPE INNER RADIUS    PIPE OUTER RADIUS    ',
     *' FIN HEIGHT   ')
1031  FORMAT(4X,F8.5,' M',11X,F8.5,' M',5X,F10.5,' M')
1032  FORMAT(/' FIN SPACING          FIN WIDTH    ',
     *' CONDENSATE HEIGHT  ')
1033  FORMAT(1X,F8.5,' M',10X,F8.5,' M',7X,F9.8,' M')
1034  FORMAT(/' TEMPERATURE INSIDE PIPE     TEMPERATURE ',
     *' OUTSIDE CONDENSATE LAYER ')
1035  FORMAT(7X,F4.1,' C',34X,F4.1,' C')
1036  FORMAT(/' K METAL          K LIQUID      H INSIDE PIPE ',
     *' H IN CONDENSATE LAYER')
1037  FORMAT(F5.0,' W/M',4X,F5.1,' W/M',3X,F10.0,' W/M**2',
     * 5X,10.0,' W/M**2')
1040  FORMAT(/' Q IN ON FIN UPPER AND SIDE SURFACES    ',
     *F9.3,' WATTS ')
1041  FORMAT(/' Q IN ON PIPE SURFACE    ',15X,F9.3,' WATTS')
1042  FORMAT(/' TOTAL Q IN THROUGH PIPE AND FIN SURFACE   ',
     *F5.3,' WATTS ')
1043  FORMAT(/' Q IN THROUGH CONDENSATE ',12X,F9.3,' WATTS')
1044  FORMAT(/' Q OUT THROUGH PIPE INNER SURFACE  ',3X,F9.3,
     *' WATTS ')
1045  FORMAT(12F6.2)
1047  FORMAT(/' Q IN THROUGH JPPER FIN SURFACE',9X,F9.3,
     *' WATTS ')
1048  FORMAT(/' Q IN THROUGH FIN SIDE SURFACE ',9X,F9.3,
     *' WATTS ')
C
C
      CLOSE(IWR,IOSTAT=ICK)
      IF(ICK .NE. 0) WRITE(IOT,1051)EEX
1051  FORMAT('TROUBLE CLOSING PRINTER OUTPUT FILE')
C
C
      STOP
      END
```

LIST OF REFERENCES

1. Wanniarachchi, A.S., Marto, P.J., and Rose, J.W., "Filmwise Condensation of Steam on Externally-Finned Horizontal Tubes," Fundamentals of Phase Change: Boiling and Condensation, HTD Vol. 38, C.T. Avedisian and T.M. Tudy (Eds.), ASME, 1984.

2. Wanniarachchi, A.S., Marto, P.J., and Rose, J.W., "Film Condensation of Steam on Horizontal Finned Tubes: Effect of Fin Spacing, Thickness and Height," Multiphase Flow and Heat Transfer, HTD Vol. 47, V.K. Dhir, J.C. Chen and D.C. Jones (Eds.), ASME, 1985, pp. 93-100.

3. Flook, F.A., Film Condensation of Steam on Externally Finned Horizontal Tubes, M.S. Thesis, Naval Postgraduate School, Monterey, California, March 1985.

4. Rudy, T.M., and Webb, R.L., "Condensate Retention of Horizontal Integral-Fin Tubes, Advances in Enhanced Heat-Transfer," 1981, HTD Vol. 18, presented at 20th National Heat-Transfer Conference, Milwaukee, Wisconsin, August 1981.

5. Honda, H., Nozu, S., Mitsumori, K., "Augmentation of Condensation on Horizontal Finned Tubes by Attaching Porous Drainage Plates," Proc. ASME-JSME Thermal Engineering Conference, Hawaii, 1983.

6. Rudy, T.M., and Webb, R.L., "An Analytical Model to Predict Condensate Retention on Horizontal, Integral-Fin Tubes," ASME/JSME Thermal Engineering Joint Conference, Vol. 1, March 20-24, 1983.

7. Rudy, T.M., and Webb, R.L., "Theoretical Model for Condensation on Horizontal, Integral-Fin Tubes," Heat Transfer, Seattle, AIChE Symp. Ser., Vol. 79, No. 225, 1983.

8. Owen, R.G., Sardesai, R.G., Smith, R.A., and Lee W.C., "Gravity Controlled Condensation on a Low-Fin Tube," Condensers: Theory and Practice, Inst. Chem. Engrs. Symp. Ser. 75, 1983.

9. Yau, K.K., Cooper, J.R., and Rose, J.W., "Effects of Fin Spacing and Drainage Strips on the Condensation Heat-Transfer Performance of Horizontal Low Integral-Fin Tubes," Fundamentals of Phase Change: Boiling and Condensation, HTD Vol. 38, C.T. Avedisian and T.M. Rudy (Eds.) ASME, 1984, pp. 151-156.

10. Beatty, B.O., and Katz, D.L., "Condensation of Vapors on Outside of Finned Tubes," Chemical Engineering Progress, Vol. 44, No. 1, January 1948.

11. Honda, H., and Nozu, S., "A Prediction Method for Heat-Transfer During Film Condensation in Horizontal Low Integral-Fin Tubes," Fundamentals of Phase Change: Boiling and Condensation, HTD Vol. 38, C.T. Avedisian and T.M. Rudy (Eds.), ASME, 1984, pp. 107-114.

12. O'Hare, M.S., The Effectiveness of Heat Exchangers With One Shell Pass and Three Tube Passes, M.S. Thesis, Naval Postgraduate School, Monterey, California, Juen 1985.

13. Kern, D.Q. and Kraus, A.D., Extended Surface Heat Transfer, McGraw-Hill Book Company, New York, NY, 1972.

INITIAL DISTRIBUTION LIST

		No. Copies
1.	Defense Technical Information Center Cameron Station Alexandria, Virginia 22304-6145	2
2.	Library, Code 0142 Naval Postgraduate School Monterey, California 93943-5100	2
3.	Department Chairman, Code 69Mx Department of Mechanical Engineering Naval Postgraduate School Monterey, California 93943-5100	1
4.	Mr. Andrew Gomori 15 Woodview Avenue Fords, New Jersey 08863	1
5.	Friendship Library Fairleigh Dickenson University Madison, New Jersey 07940	1
6.	Professor A.D. Kraus, Code 69Ks Department of Mechanical Engineering Naval Postgraduate School Monterey, California 93943-5100	2
7.	Lt. Michael A. Gomori 15 Woodview Avenue Fords, New Jersey 08863	2
8.	Dr. A.S. Wanniarachchi, Code 69Wa Department of Mechanical Engineering Naval Postgraduate School Monterey, California 93943-5100	1

END

FILMED

3-86

DTIC